ENGINEERING OF
BIOMATERIALS
INŻYNIERIA BIOMATERIAŁÓW
JOURNAL OF POLISH SOCIETY FOR BIOMATERIALS AND FACULTY OF MATERIALS SCIENCE AND CERAMICS AGH-UST
CZASOPISMO POLSKIEGO STOWARZYSZENIA BIOMATERIAŁÓW I WYDZIAŁU INŻYNIERII MATERIAŁOWEJ I CERAMIKI AGH

Number 142
Numer 142
Volume XX
Rok XX

OCTOBER 2017
PAŹDZIERNIK 2017

ISSN 1429-7248

PUBLISHER:
WYDAWCA:

Polish Society for Biomaterials in Krakow
Polskie Stowarzyszenie Biomateriałów w Krakowie

EDITORIAL COMMITTEE:
KOMITET REDAKCYJNY:

Editor-in-Chief
Redaktor naczelny
Jan Chłopek

Editor
Redaktor
Elżbieta Pamuła

Secretary of editorial
Sekretarz redakcji
Design
Projekt
Katarzyna Trała
Augustyn Powroźnik

ADDRESS OF EDITORIAL OFFICE:
ADRES REDAKCJI:

AGH-UST
30/A3, Mickiewicz Av.
30-059 Krakow, Poland
Akademia Górniczo-Hutnicza
al. Mickiewicza 30/A-3
30-059 Kraków

Issue: 250 copies
Nakład: 250 egz.

Scientific Publishing House AKAPIT
Wydawnictwo Naukowe AKAPIT
e-mail: wn@akapit.krakow.pl

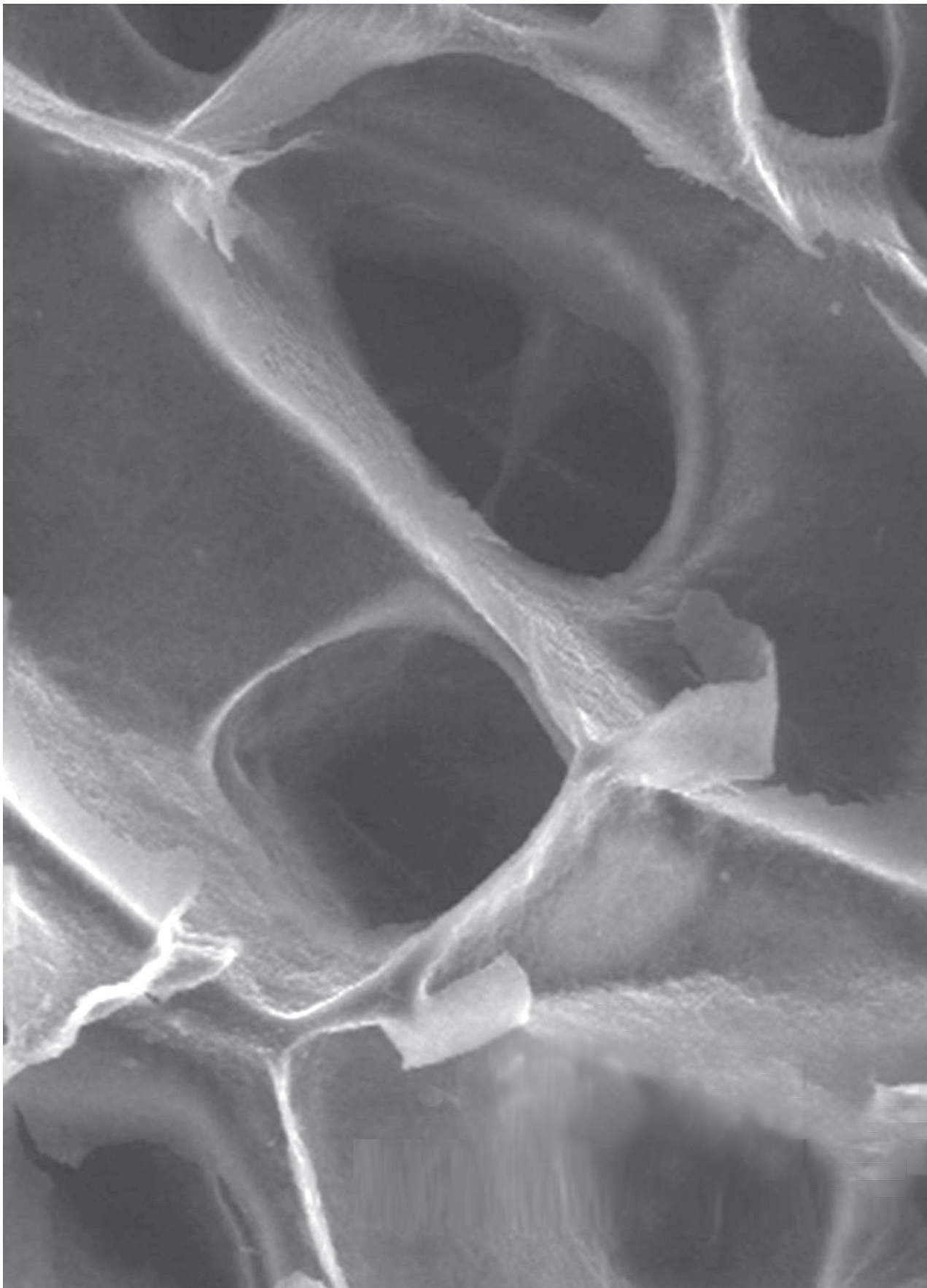

ENGINEERING OF
BIOMATERIALS

EDITORIAL BOARD
KOMITET REDAKCYJNY

INTERNATIONAL EDITORIAL BOARD
MIĘDZYNARODOWY KOMITET REDAKCYJNY

ENGINEERING OF BIOMATERIALS

Wskazówki dla autorów

1. Prace do opublikowania w kwartalniku „Engineering of Biomaterials / Inżynieria Biomateriałów" przyjmowane będą wyłącznie z tłumaczeniem na język angielski. Obcokrajowców obowiązuje tylko język angielski.
2. Wszystkie nadsyłane artykuły są recenzowane.
3. Materiały do druku prosimy przysyłać na adres e-mail:kabe@agh.edu.pl.
4. Struktura artykułu:
• TYTUŁ • Autorzy i instytucje • Streszczenie (200-250 słów) • Słowa kluczowe (4-6) • Wprowadzenie • Materiały i metody • Wyniki i dyskusja • Wnioski • Podziękowania • Piśmiennictwo
5. Autorzy przesyłają pełną wersję artykułu, łącznie z ilustracjami, tabelami, podpisami i literaturą w jednym pliku. Ilustracje, tabele, podpisy i literatura powinny być umieszczone również w wersji angielskiej. Artykuł w tej formie przesyłany jest do recenzentów. Dodatkowo autorzy proszeni są o przesłanie materiałów ilustracyjnych (rysunki, schematy, fotografie, wykresy) w oddzielnych plikach (format np. .jpg, .gif., .tiff, .bmp). Rozdzielczość rysunków min. 300 dpi. Wszystkie rysunki i wykresy powinny być czarno-białe lub w odcieniach szarości i ponumerowane cyframi arabskimi. W tekście należy umieścić odnośniki do rysunków i tabel. W tabelach i na wykresach należy umieścić opisy polskie i angielskie.
6. Na końcu artykułu należy podać wykaz piśmiennictwa w kolejności cytowania w tekście i kolejno ponumerowany.
7. Redakcja zastrzega sobie prawo wprowadzenia do opracowań autorskich zmian terminologicznych, poprawek redakcyjnych, stylistycznych, w celu dostosowania artykułu do norm przyjętych w naszym czasopiśmie. Zmiany i uzupełnienia merytoryczne będą dokonywane w uzgodnieniu z autorem.
8. Opinia lub uwagi recenzentów będą przekazywane Autorowi do ustosunkowania się. Nie dostarczenie poprawionego artykułu w terminie oznacza rezygnację Autora z publikacji pracy w naszym czasopiśmie.
9. Za publikację artykułów redakcja nie płaci honorarium autorskiego.
10. Adres redakcji:

Czasopismo
„Engineering of Biomaterials / Inżynieria Biomateriałów"
Akademia Górniczo-Hutnicza im. St. Staszica
Wydział Inżynierii Materiałowej i Ceramiki
al. Mickiewicza 30/A-3, 30-059 Kraków
tel. (48) 12 617 25 03, 12 617 25 61
tel./fax: (48) 12 617 45 41
e-mail: chlopek@agh.edu.pl, kabe@agh.edu.pl

Szczegółowe informacje dotyczące przygotowania manuskryptu oraz procedury recenzowania dostępne są na stronie internetowej czasopisma:
www.biomat.krakow.pl

Warunki prenumeraty

Zamówienie na prenumeratę prosimy przesyłać na adres:
apowroz@agh.edu.pl, tel/fax: (48) 12 617 45 41
Cena pojedynczego numeru wynosi 20 PLN
Konto:
Polskie Stowarzyszenie Biomateriałów
30-059 Kraków, al. Mickiewicza 30/A-3
ING Bank Śląski S.A. O/Kraków
nr rachunku 63 1050 1445 1000 0012 0085 6001

Prenumerata obejmuje 4 numery regularne i nie obejmuje numeru specjalnego (materiały konferencyjne).

Instructions for authors

1. Papers for publication in quarterly journal „Engineering of Biomaterials / Inżynieria Biomateriałów" should be written in English.
2. All articles are reviewed.
3. Manuscripts should be submitted to editorial office by e-mail to kabe@agh.edu.pl.
4. A manuscript should be organized in the following order:
• TITLE • Authors and affiliations • Abstract (200-250 words) • Keywords (4-6) • Introduction • Materials and Methods • Results and Discussions • Conclusions • Acknowledgements • References
5. All illustrations, figures, tables, graphs etc. preferably in black and white or grey scale should be additionally sent as separate electronic files (format .jpg, .gif., .tiff, .bmp). High-resolution figures are required for publication, at least 300 dpi. All figures must be numbered in the order in which they appear in the paper and captioned below. They should be referenced in the text. The captions of all figures should be submitted on a separate sheet.
6. References should be listed at the end of the article. Number the references consecutively in the order in which they are first mentioned in the text.
7. The Editors reserve the right to improve manuscripts on grammar and style and to modify the manuscripts to fit in with the style of the journal. If extensive alterations are required, the manuscript will be returned to the authors for revision.
8. Opinion or notes of reviewers will be transferred to the author. If the corrected article will not be supplied on time, it means that the author has resigned from publication of work in our journal.
9. Editorial does not pay author honorarium for publication of article.
10. Address of editorial office:

Journal
„Engineering of Biomaterials / Inżynieria Biomateriałów"
AGH University of Science and Technology
Faculty of Materials Science and Ceramics
30/A-3, Mickiewicz Av., 30-059 Krakow, Poland
tel. (48) 12) 617 25 03, 12 617 25 61
tel./fax: (48) 12 617 45 41
e-mail: chlopek@agh.edu.pl, kabe@agh.edu.pl

Detailed information concerning manuscript preparation and review process are available at the journal's website:
www.biomat.krakow.pl

Subscription terms

Subscription rates:
Cost of one number: 20 PLN
Payment should be made to:
Polish Society for Biomaterials
30/A3, Mickiewicz Av.
30-059 Krakow, Poland
ING Bank Slaski S.A.
account no. 63 1050 1445 1000 0012 0085 6001

Subscription includes 4 issues and does not include special issue (conference materials).

ISBPPB 2018

Join the ISBPPB 2018 Conference to hear the latest research findings on polymers in medicine and enjoy many opportunities to network with colleagues and new friends from all over the world

4th International Conference on

Biomedical Polymers & Polymeric Biomaterials

15–18 July 2018, Kraków, POLAND





ISBPPB 2018 topics:

biodegradable polymers, hydrogels, polysilanes, polysaccharides, polyurethanes, polymer foams, smart polymers, shape memory polymers, polymers for dental and orthopedic applications, blood-contacting polymers, polymers for skin grafting, polymers for targeted drug delivery, polymers for tissue engineering, **and many more**

ISBPPB 2018 program:

- Plenary/Invited Lectures
- Oral Presentations
- Young Researcher Presentations
- Poster Session
- Exhibitions

www.isbppb2018.org

Polish Society for Biomaterials

Faculty of Materials Science and Ceramics AGH-UST

International Society for Biomedical Polymers and Polymeric Biomaterials

CONGRESS BUREAU JORDAN GROUP

SPIS TREŚCI

CONTENTS

Wersja papierowa czasopisma „Engineering of Biomaterials / Inżynieria Biomateriałów" jest jego wersją pierwotną
Printed version of „Engineering of Biomaterials / Inżynieria Biomateriałów" is a primary version of the journal

FUNCTIONALIZED CELLULOSE AS A MATRIX FOR THE SYNTHESIS OF LIBRARY OF MOLECULAR RECEPTORS USEFUL FOR SCREENING OF COMPOUNDS WITH ANTI-HISTAMINE ACTIVITY

Małgorzata E. Walczak*, Justyna Frączyk, Zbigniew J. Kamiński, Beata Kolesińska

Institute of Organic Chemistry,
Lodz University of Technology,
Zeromskiego 116, 90-924 Lodz, Poland
* e-mail: malgorzata.walczak@p.lodz.pl

Abstract

The library of molecular receptors was formed by self-organization of N-heptanoylated dipeptides anchored in the regular fashion via aminophenylamino-1,3,5-triazine linker to the surface of cellulose membrane. SPOT method was used for the synthesis of peptide library. As C-terminal amino acids of peptide fragments were attached: Ala, Pro and Phe, while as a N-terminal amino acids were applied all natural amino acids. DMT/NMM/TosO- was selected as a coupling reagent for synthesis of library of N-heptanoylated dipeptides. These constructs were used as a tool for distinguishing pharmaceutically active compounds acting on histamine receptors. In the studies as active compounds were tested: Doxylamine and Difenhydramine with histamine agonist activity, Ranitidine and Cimetidine with antagonist activity as well as Histamine – natural ligand. The binding of colourless ligands was monitored by staining with Brilliant Black used as reporter dye and quantitative colour measurement was performed in 256 grade gray scale by using Image-Quant software. Substantial differences in the ability of interactions of agonists and antagonists with bounding pockets were observed with selected molecular receptors. From 60 elements library of molecular receptors were selected 12, which were able to distinguish between agonists or antagonists. It has been found that even small changes (Leu residue vs Val residue) in the structure of molecular receptor influenced specificity of agonist or antagonist binding.

Keywords: *molecular receptors, immobilized peptides, binding pocket, agonist/antagonist, histamine receptors*

[Engineering of Biomaterials 142 (2017) 2-6]

Introduction

Cellulose is a biopolymer composed of β D-glucopyranose residues bonded with 1,4 glycosidic bonds. Its characteristic feature is the equatorial arrangement of C2, C3 secondary hydroxyl groups and the primary C6-hydroxylmethyl group. The CH_2OH group is in trans-gauche position with respect to O5-C5 and C4-C-5 bonds. The result of this arrangement is the regular structure of cellulose resulting from the high content of crystalline phase and small content of the amorphous one. Cellulose has four allomorphic forms: I (Iα, Iβ), II, III, IV. Cellulose I and cellulose II form the crystalline phase. In both cases, the presence of hydrogen bonds between the O3-H ---- O5 within the chain causes the formation of rigid linear chains. The differences between both allomorphic forms of cellulose depend on the antiparallel arrangement of chains of cellulose II and on the occurrence of additional hydrogen bonds. For cellulose I, a hydrogen bond is between O6-H ---- O3 and in the case of cellulose II this bond is formed between O6-H ---- O2 [1]. Another great advantage of cellulose is the precisely defined reactivity of hydroxyl groups in each subsequent chain. It is generally assumed that primary hydroxyl groups are about 25 times more reactive than secondary ones [2]. It is also important that cellulose is readily available, both as the most abundant material produced by plants and microbes. Different origin of cellulose is causing this material available in different forms, ranging from nano-, micro- to biocellulose [3-5]. Regardless of the origin of cellulose, the procedures for reducing amorphous areas by hydrolysis are crucial to the properties of the biopolymer. Presented facts make cellulose and its derivatives widely applicable. The most sophisticated are application on chiral stationary phases [6], diaphragms used in filtration [7], membranes used in SPOT technology [8] up to the application as components of drugs formulation and drug delivery systems [9,10].

Recently, it has been shown that cellulose can be used as a support for anchoring on its surface *N*-lipidated peptides, which are forming binding cavities mimicking natural receptors and/or enzymes [11,12]. The key factor to achieve enzymatic activity or ligand binding capacity is the dynamic adaptation of peptide chains forming molecular receptors, by induced conformational changes, to the shape of the bounded ligand [13]. Two factors are crucial for efficient ligand binding: the space between immobilized peptides and the presence of elements offering most of weak interactions including π-acceptor, π-donor, van der Waals forces, hydrophobic interactions, ionic bonds and hydrogen bonds [14]. The interactions between binding pocket and docked ligand are highly selective and binding cavities are able to differentiate ligands recognizing their size, shape, charge distribution, chirality and polarity. High selectivity of interactions between molecular receptor and ligand is very important because the biological activity can be determined by even small changes in the ligand structure. The binding strength of ligands through the molecular receptors is the outcome of all interactions between the host and the guest and depends on both the structures of the ligand and the molecular receptor. The process of binding is reversible due to the nature of weak interactions between ligands and the binding pockets (FIG. 1).

Additionally, it has been found that the mechanism of binding is competitive and therefore the described process is mimicking the interactions involving natural receptors. This inspired us to use molecular receptors as tools for the testing of pharmacologically active compounds. The goal of these studies was to test whether a library of molecular receptors formed by self-organization of peptides immobilized on cellulose can mimic a histamine receptor and thus be useful in evaluation antihistamine active compounds diversifying their mode of action. It has been expected that it would be possible to select molecular receptors selectively interacting with agonists and antagonists.

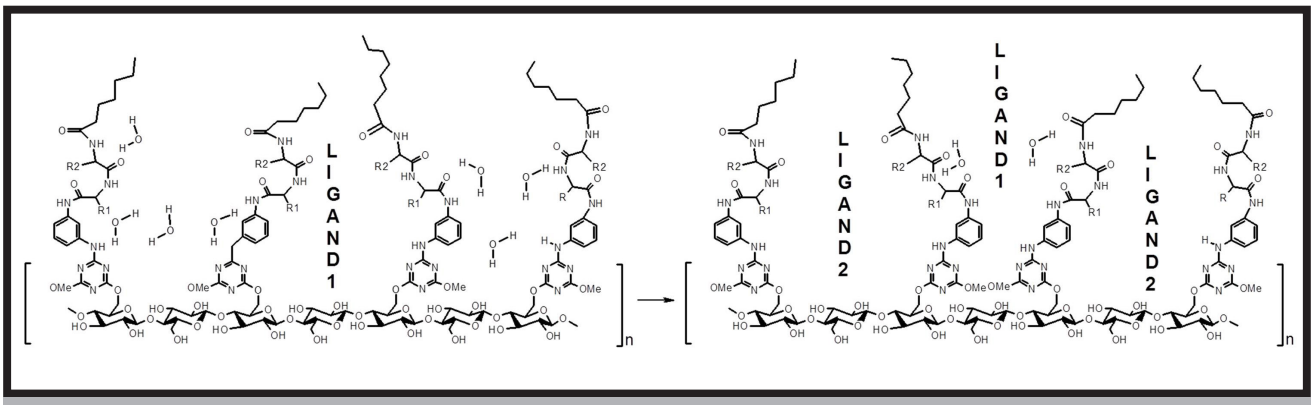

FIG. 1. Competitive, reversible mechanism of docking ligands into binding pockets.

Materials and Methods

General information

During the synthesis were used: tetrahydrofuran (THF), dichlormethan (DCM), methanol (MeOH) (POCH, 99.8%); N,N-dimethylformamid, (DMF) (J.T.Baker, 99.9%); 1-methyl-2-pyrrolidinone, (NMP) (Acros Organics, >99.5%); Piperidine, (SAFC, >99%); 4-methylmorpholine, (NMM) (Alfa Aesar, 99%); all Fmoc-protected amino acids (GL Biochem, >98.5%); 4-(4,6-dimethoxy-1,3,5-triazin-2-yl)-4-methylmorpholinium 4-toluenesulfonate (DMT/NMM/ $TosO^-$) prepared according optimized procedure [15], Histamine, Diphenhydramine, Doxylamine, Cimetidine, Ranitidine, Brilliant Black BN (tetrasodium (6Z)-4-acetamido-5-oxo-6-[[7-sulfonato-4-(4-sulfonatophenyl)azo-1-naphthyl]hydrazono] naphthalene-1,7-disulfonate) (Sigma Aldrich, >98%).

Immobilization of 2,4-dichloro-6-methoxy-1,3,5-triazine (DCMT): 6 sheets (10 cm x 15 cm) of Whatman-7 filter paper were immersed in 1M NaOH (40 ml) and gently shaken for 15 min. An excess of solution was removed, then the wet paper sheets were soaked in suspension of finely grounded sodium bicarbonate in 1M solution of 2,4-dichloro-6-methoksy-1,3,5-triazine (DCMT) (6.8 g) in THF (40 ml) and again gently shaken for 60 min at room temperature (rt). Then cellulose sheets were washed with THF (2 x 30 ml), acetone (2 x 30 ml), acetone:H_2O 1:1 (2 x 40 ml), acetone (2 x 40 ml) and with DCM (30 ml), than left to remove the remaining solvent and dried in a vacuum desiccator. Elemental analysis for cellulose was found: %N 0.00-0.05 and %Cl 0.01-0.05, after DCMT immobilization it was found: %N 3.64 and %Cl 2.66. Loading of the cellulose sheets with triazine was calculated from elemental analysis data. Surface loading calculated according to nitrogen content was $31.9 \cdot 10^{-6}$ mol (N)/cm^2; which was equivalent to $NL^s = 10.6 \cdot 10^{-6}$ mol (triazine)/cm^2 and $CIL^s = 9.2 \cdot 10^{-6}$ mol (Cl)/cm^2.

Immobilization of m-phenylenediamine: The cellulose sheets functionalized with DCMT were immersed in 1 M solution of *m*-phenylenediamine (4.3 g) in THF (40 ml) and gently shaken for 24 h at rt. Then sheets were washed successively with THF (2 x 20 ml), DMF (2 x 20 ml), again THF (2 x 20 ml) and dried in desiccator.

SPOT synthesis of N-hepatnoyled peptides on the cellulose: The peptides were performed on automatic synthesizer ResPep SL by Intavis using SPOT synthesis. The 0.56 M solutions of all Fmoc-protected natural amino acids were prepared in NMP. As a coupling reagent was used a 0.5 M solution of 4-(4,6-dimethoxy-1,3,5-triazin-2-yl)-4-methylmorpholinium 4-toluenesulfonate (DMT/NMM/$TosO^-$) in DMF. As a base 2 M NMM in DMF was used. To remove Fmoc protecting group 25% piperidine in DMF was used. *The first synthetic cycle included*: Preactivation: 6 min, for each spot: 0.15 µl solution of coupling reagent; 0.073 µl solution of NMM; 0.17 µl amino acid (Fmoc-Ala-OH, Fmoc-Pro-OH, Fmoc-Phe-OH); 0.003 µl NMP; Coupling: 2 x 3 min; for each coupling was used 0.198 µl of preactivated solution. *The second synthetic cycle included*: Fmoc-group deprotection (2 x 10 min, dispense volume: 500 µl); Preactivation: 6 min, for each spot: 0.15 µl solution of coupling reagent; 0.073 µl solution of NMM; 0.17 µl amino acid (all natural amino acids); 0.003 µl NMP; Coupling: 2 x 3 min; for each coupling is used 0.198 µl of preactivated solution. *The third synthetic cycle included*: Fmoc-group deprotection (2 x 10 min, dispense volume: 500 µl); Coupling: 1 x 7.5 min; for each spot were used: 0.3 µl NMP and 0.15 µl of 0.25 M solution of triazine esters of heptanoic acid in DMF:NMP (1:1).

Deprotection of the side chains of dipeptides: Modified cellulose membranes were treated with mixture consisting of 50% (v/v) trifluoroacetic acid in DCM (200 ml) with 3% (v/v) water and 2% (v/v) trisopropylsilane for 5 h. Then the membranes were washed with DCM (2 x 100 ml), EtOH (2 x 100 ml) and dried in a vacuum desiccator.

Buffering of cellulose membranes: The modified cellulose membrane were buffered with phosphate buffer pH 7.0 (200 ml) for 30 min. Then, the celluloses were washed with water (2 x 200 ml) and with mixture MeOH : H_2O (1:1) and dried to constant weight in the vacuum dessicator. During the synthesis two identical libraries were synthesized on each functionalized sheet, after splitting each sheet for two parts, one of them was treated with active substance and then with Brilliant Black, the second one was reared with the reporter dye only.

The docking of active substances to the binding pockets of library N-heptanoyled peptides immobilized on the cellulose: The cellulose sheets were treated with 10 ml 0.002 M solution of active substances: Histamine, Diphenhydramine, Doxylamine, Cimetidine, Ranitidine. After 30 min the excess of the solution was removed and the sheets were washed with MeOH (5 x 100 ml). After drying to the constant weight, the cellulose sheets were treated with 1.25 mM solution of the Brillant Black in MeOH for 30 min. Then the solution was removed and sheets were washed with MeOH (8 x 100 ml). Cellulose membranes after staining were dried in vacuum desiccator, scanned and processed using ImageQuant program. Ability of molecular receptors to interact with colourless active compounds was calculated as difference in intensity of coloration caused by docking reporter dye and intensity of coloration after treatment with colourless ligand and subsequently with reporter dye. In this way, for each spot average value of “gray” coloration corresponding to interaction between binding pocket of molecular receptor and antihistamine ligand was determined.

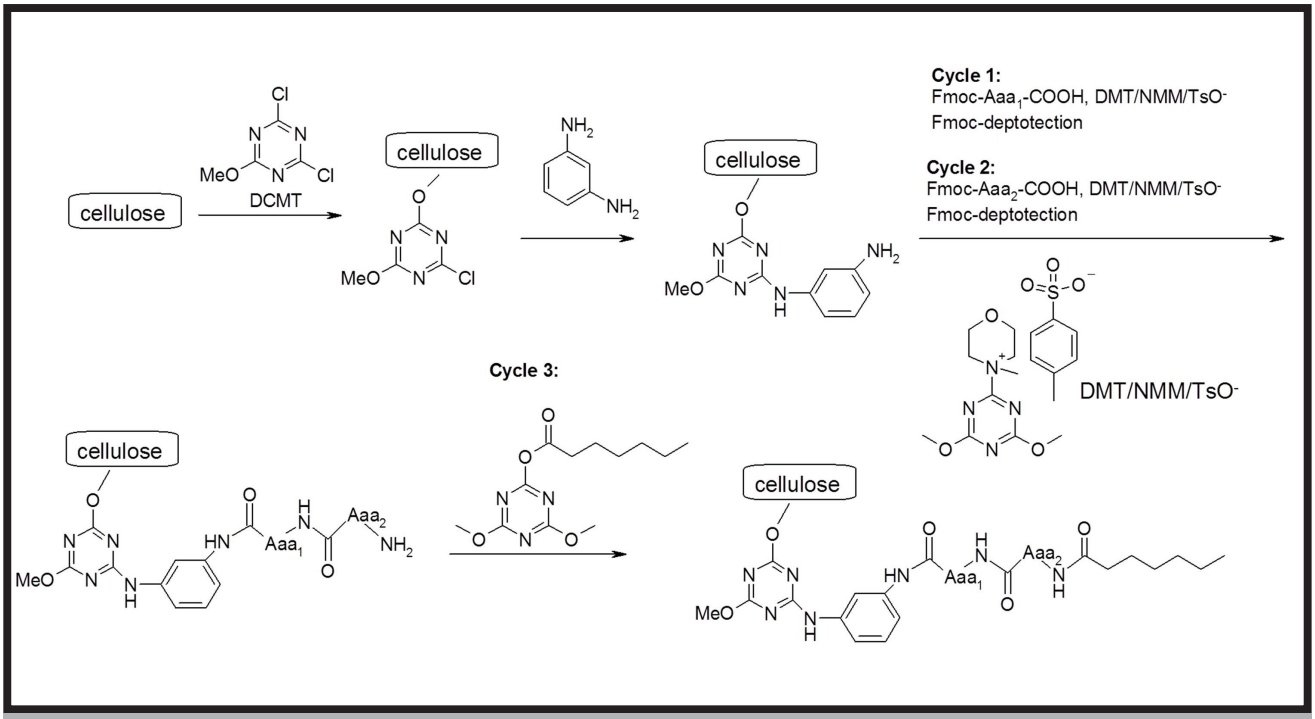

FIG. 2. Synthetic pathway for preparation of *N*-heptanoylated dipeptides immobilized on cellulose.

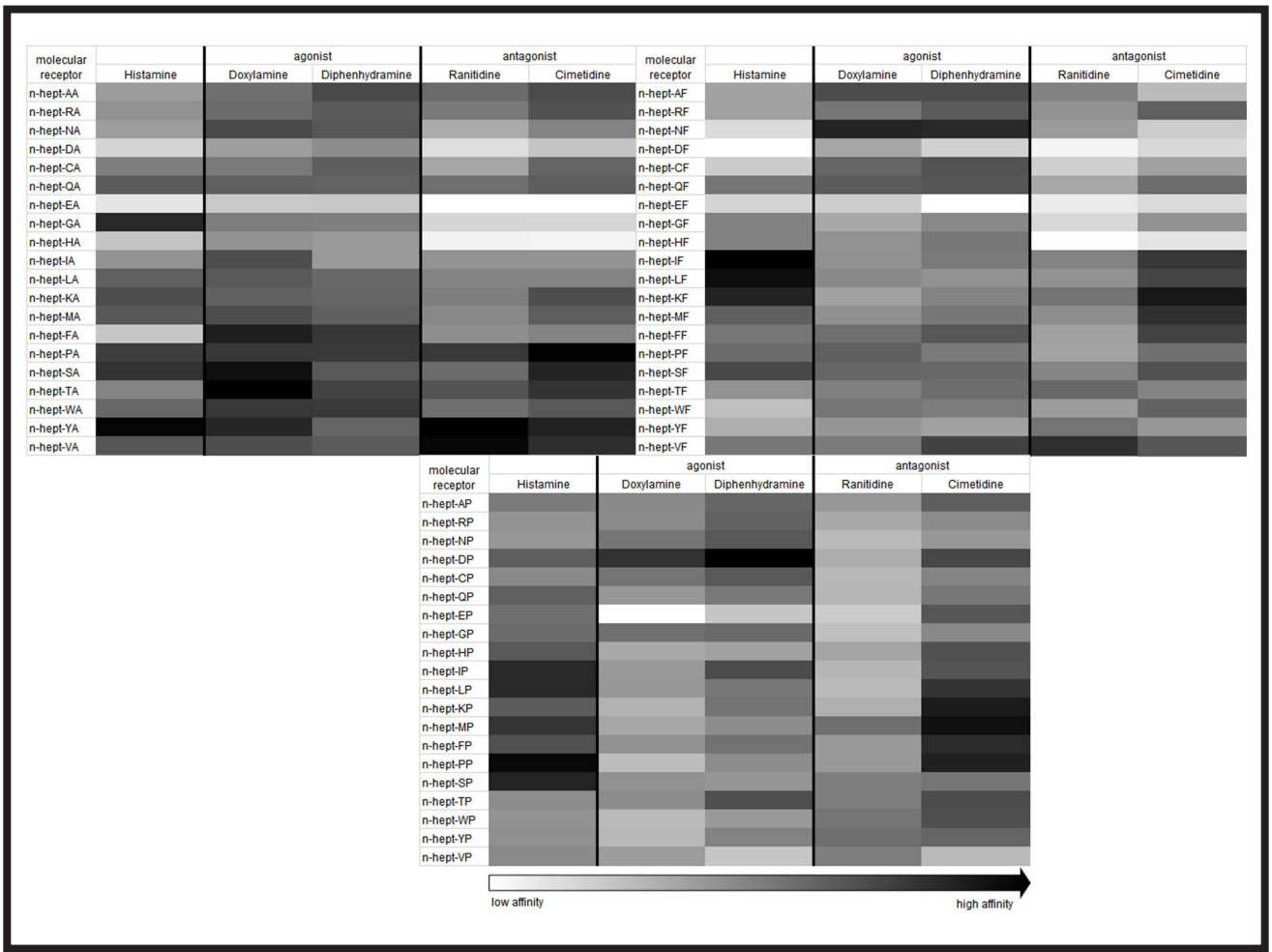

FIG. 3. The map of intensity of bounding of tested compounds by cavities of library of molecular receptors immobilized on cellulose, dark coloration - strong molecular complex, light coloration - weak molecular complex.

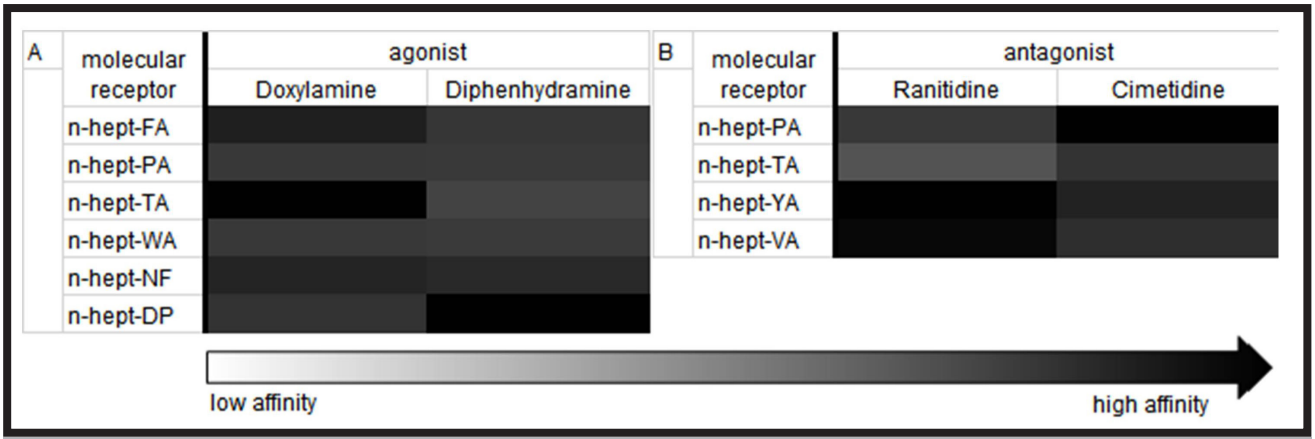

FIG. 4. The map of intensity of bounding of tested compounds by selected molecular receptors giving strong molecular complexes.

Results and Discussions

In the study all natural amino acids were used as substrates for the synthesis of a library of molecular receptors. A randomized approach to design the peptide fragments was preferred due to complexity of the search for molecular receptors capable of differentiating affinity of agonists and antagonists of histamine receptors. The molecular receptors were prepared using a stepwise process involving functionalization of cellulose with a 2,4-dichloro-6-methoxy-1,3,5-triazine derivative followed by reaction with *m*-phenylenediamine, coupling with *N*-Fmoc protected Ala, Pro or Trp, deprotection of the *N*-terminus, coupling with all Fmoc protected proteinogenic amino acids, and finally acylation with *n*-heptanoic acid (FIG. 2). Synthesis of *N*-heptanoylated dipeptides attached on the surface of the modified cellulose membrane was done by using the automated SPOT technique. 4-(4,6-Dimethoxy-1,3,5-triazin-2-yl)-4-methylmorpholinium 4-toluenesulfonate (DMT/NMM/$TosO^-$), a coupling reagent with well documented efficiency in peptide synthesis, was applied [15]. Doxylamine and Difenhydramine with histamine agonist activity, Ranitidine and Cimetidine with antagonist activity as well as Histamine – the natural ligand, were used in the studies involving molecular receptors acting as a histamine receptors model.

Using a competitive mechanism of ligand binding to cavities of molecular receptors, it was possible to visualize molecular complexes formed with colourless ligands applying the procedure with reporter dye [16].

The ability of molecular receptors to interact with colourless active compounds was calculated as a difference in intensity of coloration caused by docking reporter dye only and intensity of coloration after treatment the docked colourless ligand with the reporter dye. In this way, bigger difference in the coloration corresponded to stronger binding of ligand by receptor. This was finally presented on the interactions map by more dark “gray” coloration. Brilliant Black was used as the reporter dye. This dye was selected because it gave fairly uniform coloration of most receptors, weakly depended on the structure of the binding pocket. The observed intensity of coloration of spots corresponded to the stability and the strength of the molecular complexes formed between bounding cavities of molecular receptor and docked ligand. FIG. 3 shows the interaction map of the molecular receptor library with tested anti-histamine active compounds. It has been found that even a randomized library of *N*-heptanoylated dipeptides evidenced a significantly different susceptibility to docked pharmaceutically active compounds. The ten molecular receptors forming strong molecular complexes with both agonists and antagonists were selected and presented in FIG. 4.

Structural analysis of selected molecular receptors has indicated that in 8 out of 10 cases, the *C*-terminal amino acid of the peptide was alanine. With regard to the structure of *N*-terminal amino acid, there was a considerable variation as follow. Both aromatic amino acids, as well as hydrophobic aliphatic amino acid, and even amino acids with hydroxyl functions in the side chains were identified. Taking into account that all docked derivatives are amines, it has to be underlined that only in one case the molecular receptors contained amino acid with a carboxylic function in the side chain (Asp-Pro). This result indicates that a rather mutual adjustment between guest-host by using hydrophobic interaction and/or π-interactions is critical for the formation of stable molecular complexes. Ionic bond between the carboxyl group in the side chain of the dipeptide and the amine function of the docked ligand appear less crucial. Most important for this study was to search for molecular receptor structures for which the ability to interact would be different for agonists and antagonists, that is, depended on the biological activity of ligands. It has been found that even in the model library of molecular receptors it was possible to find such structures (FIG. 5). The observed differences in stability of molecular complexes formed with agonists and antagonists were statistically significant.

From the pool of 60 molecular receptors, 12 dipeptides were capable of distinguishing between agonists and antagonists, based on the formation of molecular complexes of substantially different stabilities. For molecular receptors with a high affinity for antagonists, the predominant residue at the *C*-terminal position of peptides was proline, while *N*-terminal amino acids residue were hydrophobic. For a pool of molecular receptors with higher affinity for agonists, in most cases at the *C*-terminal alanine residue was present. Particularly noteworthy are four molecular receptors: LeuAla, ValAla, TrpAla, TrpPro. In the case of receptor containing LeuAla there was observed higher affinity toward agonist, whilst changing leucine residue for valine (ValAla) altered the specificity toward antagonist. The similar situation was observed for TrpAla and TrpPro, exchanging *C*-terminal amino acid residues gave the receptor with different affinity against agonist or antagonist.

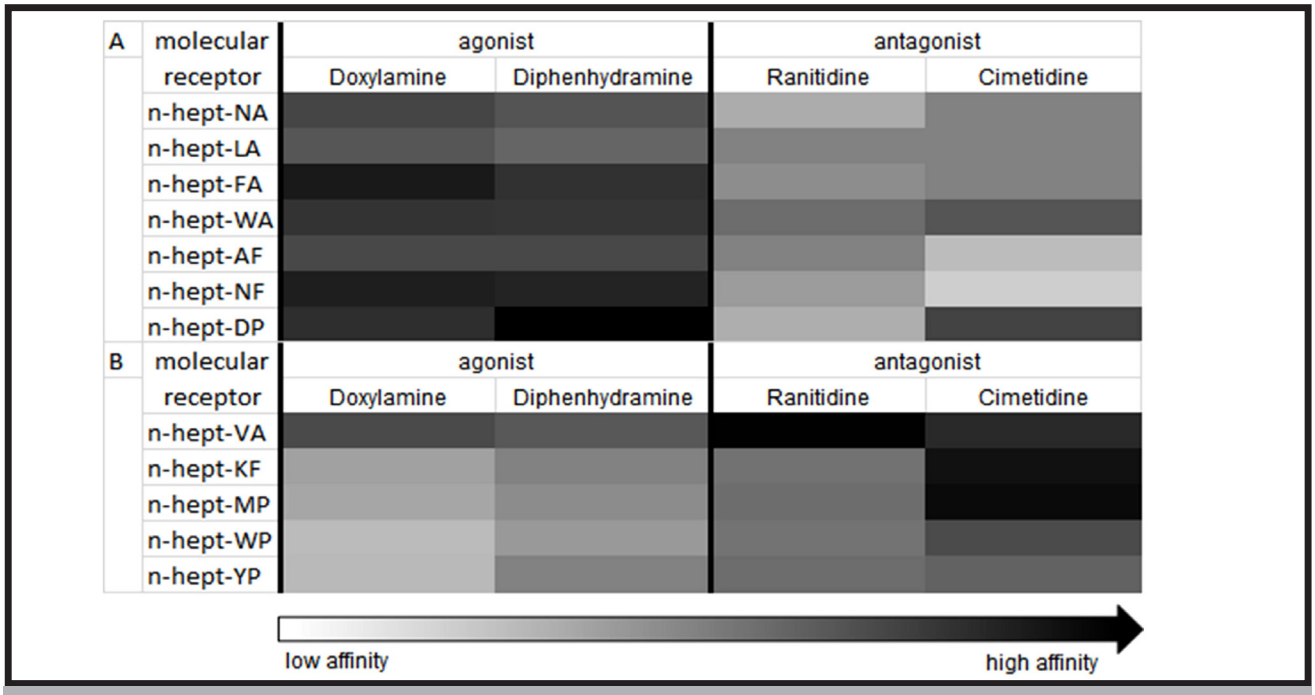

FIG. 5. The map of intensity of bounding of tested compounds by molecular receptors distinguishing agonists from antagonists.

Conclusions

These studies revealed that the library of molecular receptors is recognizing and differentiating agonistic/antagonistic profile of antihistamine active compounds. Even not understanding of complex relations between the structure of the molecular receptor and structure of the pharmacologically active substance, this should allow the construction of a new research tool useful as a platform for screening of new antihistamine compounds. Works on the synthesis of a second generation molecular receptors library based on selected molecular receptor structures and constitutive histamine H1-H4 receptor fragments are underway.

Acknowledgments

The research work is supported by Grant UMO-2016/21/N/ST5/01265.

References

[1] Langan P., Nishiyama Y., Chanzy H.: X-ray Structure of Mercerized Cellulose II at 1 Å Resolution. Biomacromolecules 2 (2001) 410-416.
[2] Klemm D., Heublein B., Fink H.P., Bohn A.: Cellulose: fascinating biopolymer and sustainable raw material. Angew. Chem. Int. Ed. 44 (2005) 3358-3393.
[3] Huang Y., Zhu C., Yang J., Nie Y., Chen C., Sun D.: Recent advances in bacterial cellulose. Cellulose 21 (2014) 1-30.
[4] Wang B., Lv X., Chen S., Li Z., Sun X., Feng C., Wang H., Xu Y.: In vitro biodegradability of bacterial cellulose by cellulase in simulated body fluid and compatibility in vivo. Cellulose 23 (2016) 3187-3198.
[5] Lu P., Hsieh Y.-L.: Preparation and properties of cellulose nanocrystals: Rods, spheres, and network. Carbohydrate Polymers 82 (2010) 329-336.
[6] Beesley T.E.: Review of Chiral Stationary Phase Development and Chiral Applications. LCGC Europe 24 (2011) 270-276.
[7] Voisin H., Bergström L., Liu P., Mathew A.P.: Nanocellulose--Based Materials for Water Purification. Nanomaterials 7 (2017) doi:10.3390/nano7030057.
[8] Kai H.K., Winkler D.F.H., Hancock R.E.W.: Peptide arrays on cellulose support: SPOT synthesis, a time and cost efficient method for synthesis of large numbers of peptides in a parallel and addressable fashion. Nature Protocols 2 (2007) 1333-1349.
[9] Almeida I.F., Pereira T., Silva N.H.C.S., Gomes F.P., Silvestre A.J.D., Freire C.S.R., et al.: Bacterial cellulose membranes as drug delivery systems: An in vivo skin compatibility study. European Journal of Pharmaceutics and Biopharmaceutics 86 (2014) 332-336.
[10] Kamel S., Ali, N., Jahangir K., Shah S. M., El-Gendy A. A.: Pharmaceutical significance of cellulose: a review. Express Polym. Lett. 2 (2008) 758-778.
[11] Fraczyk J., Kolesinska B., Kaminski Z.J.: N-lipidated oligopeptides immobilized on cellulose as new type of organocatalysts. Comb. Chem. & HTS 16 (2013) 562-571.
[12] Bak A., Daszykowski M., Kaminski Z.J., Kiec-Kononowicz K., Kuder K., Fraczyk J., Kolesinska, B., Ciosek P., Polanski J.: Probing an artificial polypeptide receptor library using a series of novel histamine H3 receptor ligands. Comb. Chem. & HTS 17 (2014) 141-156.
[13] Fraczyk J., Kaminski Z.J.: Design, synthesis, and application of a library of supramolecular structures formed by N-lipidated peptides immobilized on cellulose. Artificial receptors. J. Comb. Chem. 10 (2008) 934-940.
[14] Fraczyk J., Mrozek A., Kaminski Z.J.: Structure-activity relationship in binding ligands to library of artificial receptors: the search for biocompatible sensor. Bioelectrochemistry 80 (2010) 2-9.
[15] Kolesinska B., Rozniakowski K.K., Fraczyk J., Relich I., Papini A.M., Kamiński Z.J.: The Effect of Counterion and Tertiary Amine on the Efficiency of N-Triazinylammonium Sulfonates in Solution and Solid-Phase Peptide Synthesis, Eur. J. Org. Chem. (2015) 401-408.
[16] Nguyen B.T., Anslyn E.V.: Indicator- Displacement Assays. Coord. Chem. Rev. 250 (2006) 3118-3127.

COMPARATIVE STUDY OF BIORESORBABLE MEMBRANES „COLLAPAN" AND „COLLOST" FOR THE PREVENTION OF LOWER JAW ATROPHY

Irina Pohodenko-Chudakova[1]*, Katsiaryna Maksimovich[2]

[1] Belarusian State Medical University,
Department of Oral Surgery,
9 Kossmonavtov Str., PO Box 286, Minsk 220025,
Republic of Belarus
[2] Belarusian State Medical University,
Department of Oral Surgery,
39/167 Prityckogo Str., Minsk 220121,
Republic of Belarus
* e-mail: ip-c@yandex.ru

Abstract

Prevention of the alveolar bone atrophy represents one of the urgent problems in oral and maxillofacial surgery. The aim of the study was comparative evaluation of two osteoplastic bioresorbable membranes: "Collapan" made of collagen type II, hydroxyapatite and gentamycin sulphate, and "Collost" made of collagen type I for prevention of the mandible atrophy. 42 male patients aged from 45 to 70 years were involved in the clinical trial. Group 1, which was the reference group, included 20 individuals, in whom "Collapan" membrane was implanted to prevent atrophy of the alveolar bone. Group 2 included 22 patients, in whom "Collost" membrane with the same purpose was used. Clinical efficacy was assessed by analysis of the number of complications in the postoperative period. The level of the alveolar bone atrophy was assessed at the long-term follow-up (after 1 year) based on the parameters of the mandibular bone tissue determined by cone-beam computed tomography. In the postoperative period in the group 1 there were revealed 6 (14%) cases of infectious-inflammatory complications – alveolitis, 2 (5%) of them were revealed after the third molar atypical removal and 4 (9%) after a complicated extraction of the tooth. In group 2 – 2 (5%) complications were reviled: 1 (2.5%) - alveolitis and 1 (2.5%) - forced tooth extraction. The use of the "Collost" membrane allowed maintaining the height of the alveolar bone in patients during the observation period. The results obtained in the trial allow us to conclude that the use of the osteoplastic bioresorbable membrane "Collost" is most appropriate for prevention of the alveolar part of the lower jaw atrophy.

Keywords: *bioresorbable membrane, alveolar bone atrophy, Collost, Collapan*

[Engineering of Biomaterials 142 (2017) 7-10]

Introduction

Nowadays, prevention of alveolar bone atrophy is one of the urgent problems in oral and maxillofacial surgery [1,2]. This problem is determined by number of factors. Firstly, the significant spread of benign tumours and tumour-like bone diseases that reaches 84% of the total number of all primary bone tumour lesions [3,4]. At the same time, verification of these neoplasms of the bones of the facial skeleton constitutes a rather frequent phenomenon [5,6]. Secondly, even in the case of the absence of complications after the tooth extraction, the width of the alveolar ridge decreases during the first year in the range from 25% to 50% to the length 5-7 mm. It should be emphasized that 2/3 of the loss of this bone volume occurs during the first three months after tooth extraction. At the same period there is a significant loss of bone tissue in the vertical direction, which is usually equal to 0.9-3.25 mm [1,7,8]. Thirdly, a significant defect in bone tissue resulting in the atrophy is observed after atypical removal of the third lower molar [9,10].

Quite often such surgical intervention is complicated due to retention and dystopia of the tooth and by the lack of space in the alveolar part of the jawbone [11]. The situation can be exacerbated by the destruction of bone tissue in the region of the tooth neck and bone along the course of the root of the tooth, which is manifested by the presence of a periodically exacerbating infectious and inflammatory processes in this zone [12]. In addition, in the postoperative period, after such interventions, alveolitis may develop, which also contributes to the progression of alveolar bone atrophy. To prevent lower jaw atrophy resorbable or non-resorbable membranes can be used.

The aim of this study is a comparative evaluation of the use of two osteoplastic bioresorbable membranes "Collapan" and "Collost" for the prevention of the alveolar part of the mandible atrophy.

Materials and Methods

42 patients (men) aged 45 to 70 years were involved in the trial; they were divided into two groups by randomization. "Collapan" and "Collost" were certified by the Ministry of Health and are allowed for using in dental practice. We carried out comparative trials of the effectiveness of these membranes. These bioresorbable membranes were used in patients on clinical medical indications according Clinical treatment protocols approved by Ministry of Health. To the trial there were included persons who had no decompensated diseases in comorbidities or injuries, surgeries, connective tissue diseases, pathology of the oral mucosa and other factors that could affect the results of the study. Group 1 included 20 individuals in whom we used "Collapan" in surgical treatment to prevent atrophy of the alveolar bone. Group 2 included 22 patients in whom we used "Collost" membrane to prevent atrophy of the alveolar bone (FIG. 1).

"Collapan" (LTD Intermedapatit, Moscow, Russia) is a bioactive osteoplastic membrane being a homogeneous composition of hydroxyapatite powder, collagen type II and antibiotic (gentamicin sulphate), which is certified, approved for use in the Republic of Belarus. "Collost" (LTD Biopharma-holding, Moscow, Russia) is a membrane made of bioplastic collagen type I with a fully preserved native structure.

The patients were undergone oral surgery of atypical tooth extraction, cystectomy with apex root resection made by standard operative protocols. All patients in the postoperative period received a standard antibiotic-inflammatory therapy according treatment clinical protocol (amoxicillin, antihistamine drug loratadin, and anti-inflammatory drug ibufen).

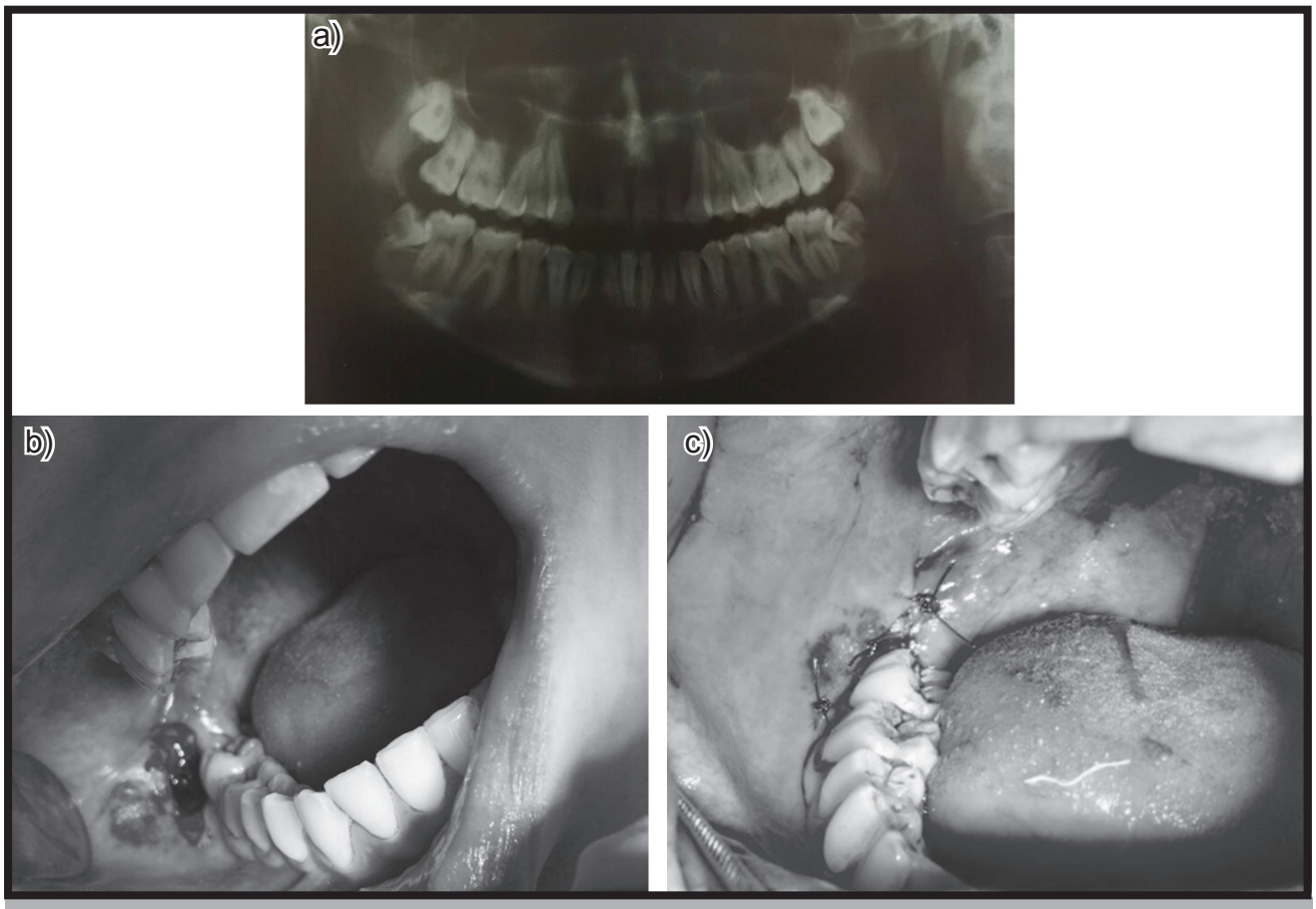

FIG. 1. Clinical case of "Collost" membrane applied in the case of dystopian wisdom tooth: a) panoramic X-ray picture, b) operative bone wound with "Collost", c) postoperative sutures.

TABLE 1. Patient distribution in groups of examination, depending on the verified diagnoses.

Verified diagnoses in patients included in the examination groups	Observation groups			
	Group 1 (n = 20, 48%)		Group 2 (n = 22, 52%)	
Radicular cyst (from one of the frontal teeth of the lower jaw)	5	25%	6	27%
		12%		14%
Chronic granulomatous periodontitis without exacerbation (molars and premolars of the lower jaw)	9	45%	9	41%
		21%		21%
Retention and dystopia of the third lower molar	6	30%	7	32%
		14%		17%
Note: the upper value (in %) is calculated in the condition that the number of patients in this group was taken as 100% for the total number of observed patients (20 and 22, respectively), the lower value (in %) is calculated on the condition that the total number of observed patients was taken as 100% (42).				

The distribution of patients in the examination groups treated with osteoplastic bioresorbable membranes "Collapan" and "Collost", depending on the verified diagnosis is presented in TABLE 1.

Clinical efficacy was assessed based on the number of complications in the postoperative period.

The level of the alveolar bone atrophy was assessed at a long-term follow-up (after 1 year) on the basis of the mandibular bone tissue parameters determined by cone-beam computed tomography (apparatus "GALILEOS"). Measurements were carried out from the results of radiological data: 1) at two symmetrical points, in the area of chewing teeth, focusing on the location of the mandibular canal (FIG. 2 – points I and II); 2) at two symmetrical points in the frontal part of the jaw, oriented to the canine line (FIG. 2 – points III and IV) [13].

The obtained data were subjected to statistical analysis using Statistica 10.0 (Version 6-Index, StatSoft Inc., USA) and Excel. Normality assumption was verified using the Shapiro-Wilk test. For data with normal distribution arithmetic mean (M) and standard deviation (σ) were calculated. When the distribution of data was different from the normal, median (Me), lower 25 quartile (LQ) and upper 75 quartile (UQ) were calculated. For comparison of two groups nonparametric Wilcoxon test and Friedman analysis of variance were performed. To assess the statistical significance between unrelated groups, the Mann-Whitney criterion (U) was used. In multiple group comparison, the Bonferoni correction was applied (p x number of comparisons). With the normal distribution of signs in the compared groups, the Student-Fisher t-criterion was used.

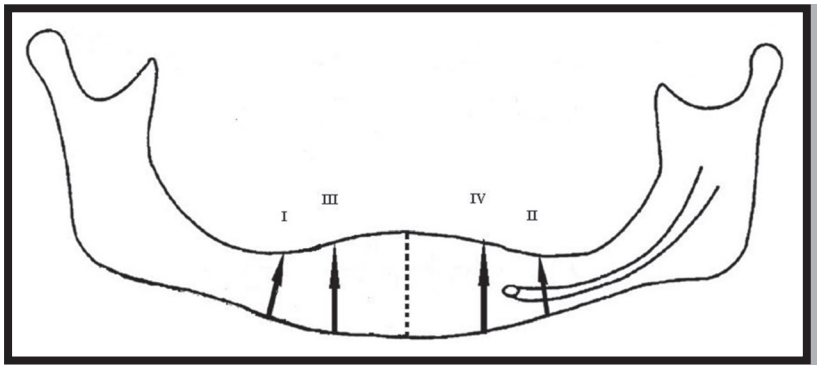

FIG. 2. Scheme of the height measurement of the lower jaw alveolar part: symmetrical points I and II are localized in the area of the chewing teeth (in determining the orientation of the mandibular canal represented in the images obtained during radiological evaluation); symmetrical points III and IV, are localized in the canine region; the dashed line indicates the middle line of the lower jaw.

TABLE 2. The data of the height and width of the alveolar part of the mandible bone of the observed groups' patients at long-term follow-up (after 1 year).

Studied parameters	Groups of examination	
	Group 1 (n = 20) Patients treated with "Collapan"	Group 2 (n = 22) Patients treated with „Collost"
Height of the alveolar ridge	11.1 (9.7−20.4) σ = ± 2.0	14.6 (11.2−22.3) σ = ± 2.2
Width of the alveolar ridge	6.2 (4.2−9.0) σ = ± 0.7	7.7 (5.1−10.2) σ = ± 0.9

Results and Discussions

In the postoperative period in the group 1, i.e. treated with "Collapan", there were six (14%) complication cases of an infectious-inflammatory nature - alveolitis: two of them (5%) were revealed after the third molar atypical removal, while four (9%) - after a complicated extraction of the tooth.

In the group 2, i.e. treated with "Collost" there were only two (5%) complication cases of an infectious and inflammatory nature: one of them (2.5%) was alveolitis as a result of the third molar atypical removal, and one (2.5%) in forced tooth extraction 11 months after the previous operation of the apex root resection of the tooth 4.5 with cystectomy. It should be emphasized that the latter complication can be attributed to the errors of endodontic preparation of the tooth before the operation. On the basis of a retrospective radiological study it was found that the root canal of the tooth 4.5 was sealed more than 5 years ago and the clinical quality control of the canal showed inappropriate canal filling but the patient did not agree to retreat the tooth 4.5.

The results of the height and width of the mandible alveolar part in patients from both groups are presented in TABLE 2.

Thus, clinical radiographic evaluation of the healing process of the post-extraction wounds and bone tissue after 1 year allowed us to come to conclusion that using of barrier membranes in oral surgery in general, optimizes the pace of reparation and regeneration due to osteoinductive and osteoconductive properties of the materials and contributes to the prevention of local atrophic processes. "Collost", i.e. the membrane made of collagen only, demonstrated more pronounced effectiveness according to received data in comparison with the membrane "Collapan", i.e. the composite hydroxyapatite-collagen membrane enriched with antibiotic.

The filling of the bone defect of the jaw bones with biocomposite materials after tooth extraction, cystectomy and other oral surgery operations is aimed at:

1. Prevention of possible complications associated with contraction and disintegration of the blood clot as well as secondary infection of the wound;

2. Acceleration of regeneration of bone tissue in the area of the defect and restoration of the shape and function of the jaw bones.

For this reason, the materials used to fill in the bone cavity after oral surgery should have a number of necessary properties. Firstly, they should be biocompatible, biodegradable and do not cause inflammatory and allergic reactions in the recipient. Secondly, they should be osteoinductive, that is, actively induce osteoblast growth and support mesenchymal stem cells to differentiate to osteogenic lineages and form bone tissue. And, thirdly, they should maintain the volume of the defect, i.e. to fulfil osteoconductive function.

To address these issues, many dentists use different biocomposite materials. Contraindications to the use of these materials are: an individual sensitivity to the drug, exacerbation of chronic diseases, impaired blood clotting, pregnancy and lactation and mucosa diseases.

The results presented in this study show advantages of using the osteoplastic bioresorbable membrane "Collost" for prevention of the mandible alveolar part atrophy. This is probably due to the fact that collagen, being a native protein, is able to easily form complexes with various drugs, including antibacterial ones. This, in turn, it allows to optimize the processes of bone tissue healing and regeneration. Application of standard anti-inflammatory therapy used in the postoperative period also diminishes atrophy of the lower jaw alveolar part in the long-term observation period. These data are consistent with the reports of D.V. Seliverstov et al. (2015) and S. D'Amato et al. (2017) [14,15].

In addition, the results show that the group of patients, which the jaw bone tissue atrophy prevention was carried out with the osteoplastic bioresorbable membrane "Collost", is the most suitable for the installation of screw dental implants.

The absence of an inflammatory response to the "Collost" application from the mucous membrane of the oral cavity and the whole organism in early postoperative period indicates a low antigenicity of this material and a high degree of its biointegration in the tissue of the recipient.

Conclusions

The results obtained in this study allow us to conclude that the osteoplastic bioresorbable membrane made of collagen type I "Collost" is more appropriate for prevention of the lower jaw alveolar part atrophy than reference membrane Collaplan made of hydroxyapatite – collagen composite enriched with gentamycin sulphate.

Acknowledgments

We are grateful to the Belarusian State University for the opportunity to conduct the research, to the "Collapan" and "Collost" companies for the materials provided.

References

[1] Andreasi B.M., Andrisani C., Lopez M.A., Gaudio R.M., Lombardo L., Carinci F.: Guided bone regeneration by means of a preformed titanium foil: A case of severe atrophy of edentulous posterior mandible. J. Biol. Regul. Homeost. Agents 30 (2 Suppl 1) (2016) 35-41.
[2] Krasny M., Krasny K., Fiedor P., Zadurska M., Kamiński A.: Long-term outcomes of the use of allogeneic, radiation-sterilised bone blocks in reconstruction of the atrophied alveolar ridge in the maxilla and mandible. Cell Tissue Bank 16(4) (2015) 631-638.
[3] Krasilnikov A.A., Nikolaev S.M., Markaryan A.A., Mondodoev A.G., Gulyaev S.M.: Influence of Collost and Collost with chymotrypsin on bone defect healing. Izvestiya Dagistani Ped. University. Natural and Exact Sci. 4, (2011) 75-79.
[4] Lima-Verde-Osterne R., Turatti E., Cordeiro-Teixeira R., Barroso--Cavalcante R.: The relative frequency of odontogenic tumors: a study of 376 cases in a Brazilian population. Med. Oral Patol. Oral Cir. Bucal. 22(2) (2017) e193-e200.
[5] Ghattamaneni S., Guttikonda V.R., Kumari M.G., Kumar D.R.: Maxillary plexiform ameloblastoma showing basaloid differentiation: report of a rare case with review of literature. Indian J. Dent. Res. 26(6) (2015) 633-636.
[6] Islamov I.M., Minenkov G.O.: To the substantiation of the choice of endoscopic removal of benign tumors of the maxillofacial region according to computed tomography data [Electronic resource], Med. Practice: 2017, Available at: http://mfvt.ru/kliniko-funkcionalnye-osobennosti-xronicheskoj-obstruktivnoj-bolezni-legkix--obuslovlennoj-vdyxaniem-pnevmotropnyx-pollyutantov-u-bolnyx--saxarnym-diabetom-2-tipa, Accessed: 22.05 2017.
[7] Avila-Ortiz G., Elangovan S., Kramer K.W., Blanchette D., Dawson D.V.: Effect of alveolar ridge preservation after tooth extraction: a systematic review and meta-analysis. J. Dent. Res. 93(10) (2014) 950-958.
[8] Hong C.E., Lee J.Y., Choi J., Joo J.Y.: Prediction of the alveolar bone level after the extraction of maxillary anterior teeth with severe periodontitis. J. Periodontal. Implant. Sci. 45(6) (2015) 216-222.
[9] Wiśniewska I., Slósarczyk A., Myśliwiec L., Sporniak-Tutak K.: Lincomycin applied to the alveolus on TCP carrier and its effect on wound healing after surgical extraction of a third molar. Ann. Acad. Med. Stetin. 55(2), (2009) 59-64.
[10] Fickl S., Fischer K., Petersen N., Happe A, Schlee M., Schlagenhauf U., Kebschull M.: Dimensional evaluation of different ridge preservation techniques: arandomized clinical study. Int. J. Periodontics Restorative Dent. 137(3) (2017) 403-410.
[11] Hassan K.S., Marei H.F, Alagl A.S.: Composite bone graft for treatment of osseous defects after surgical removal of impacted third and second molars: case report and review of the literature. Oral Surg. Oral Med. Oral Pathol. Oral Radiol. Endod. 112(6) (2011) e8−e15.
[12] de Avila E.D., Filho J.S., de Oliveira Ramalho L.T., Real Gabrielli M.F., Pereira Filho V.A.: Alveolar ridge augmentation with the perforated and nonperforated bone grafts. J. Periodontal. Implant. Sci. 44(1) (2014) 33-38.
[13] Lazarenko A.V., Kan V.V., Terskikh S.A.: Estimation of the parameters of the jaw bone tissue in patients of retirement age with complete and partial absence of teeth. Kuban Sci. Med. Bull. 151(2) (2015) 93-97.
[14] Seliverstov D.V., Kuznecov A.V., Masevnin V.V., Kondrus I.V., Novikov L.A., Yudin V.A., Sachin V.P.: The use of the biomaterial "Collost" in the complex surgical treatment of pressure ulcers of the IV degree. Rus. Med. J.: 13 (2015) 776-780.
[15] D'Amato S., Tartaro G., Itro A., Santagata M.: Mandibular bone regeneration after bone slat technique. Ann. Stomatol. (Roma) 8(1) (2017) 39-44.

GRAPHENE OXIDE AND GREEN-SYNTHESIZED REDUCED GRAPHENE OXIDE IN CHITOSAN-BASED NANOCOMPOSITES

Karolina Kosowska*, Patrycja Domalik-Pyzik, Jan Chłopek

AGH University of Science and Technology,
Faculty of Materials Science and Ceramics,
Department of Biomaterials and Composites,
Al. Mickiewicza 30, 30-059 Krakow, Poland
* e-mail: kosowska@agh.edu.pl

Abstract

The first part of the paper concerns synthesis and characterization of two types of nanomaterials: graphene oxide (GO) prepared by modified Marcano method and reduced graphene oxide (rGO) synthesized using green reductant, L-ascorbic acid. Their structural properties were investigated by attenuated total reflection Fourier-transform infrared spectroscopy (ATR-FTIR) and X-ray diffraction (XRD). Results confirmed that L-ascorbic acid is an effective reducing agent. Intensity of the oxygen-groups decreased dramatically what resulted in reduction of the GO interlayer spacing from 0.8 nm to 0.4 nm. The second part of the research was concentrated on the properties of chitosan nanocomposites modified with GO and rGO. Films were prepared by mixing of the chitosan solution with the nanoparticles dispersion. Scanning electron microscopy (SEM) was used to investigate the microstructure of the composites surface. In addition, wettability and pore size of the freeze-dried scaffolds were evaluated. Results of the mechanical tests (increase in Young's modulus) and structural characterization confirmed that chitosan solution and GO dispersion can be mixed homogeneously. Reduction of GO during composite synthesis resulted in better dispersion of the nanosheets what increased surface roughness, wettability and stability in distilled water, PBS and Ringer's solution compared to composite with GO. After detailed biological examination, rGO-modified nanocomposites can be potentially applied in tissue engineering.

Keywords: *graphene oxide, reduced graphene oxide, chitosan, hydroxyapatite, biomaterial*

[Engineering of Biomaterials 142 (2017) 11-16]

Introduction

The suitability of a material for tissue engineering is determined by many factors. Tissue scaffolds have to generate proper chemical and physical signals to be potentially able to transport bioactive molecules and stimulate tissue regeneration. For this reason, researchers are increasingly investigating materials with novel properties. Significant increase in number of studies on graphene and its derivatives has been observed in recent years. Because of its unique properties graphene is a material with great application potential in biomedical field like tissue engineering [1], bioimaging [2], biosensor [3] and drug delivery [4].

Graphene is a monolayer of carbon atoms with sp^2 hybridization. Each atom has three σ-bond and one delocalized π-bond thanks to which it connects with three other atoms and creates honeycomb lattice [5]. Two-dimensional (2D) single layer of carbon, thanks to atomic structure and remarkable electron mobility, possesses great mechanical properties [6], high electrical [7] and thermal conductivity [8], large surface area, and chemical stability [9].

In practice, graphene is defined as a mono-, bi- or multi-layer of sheets. Above the number of ten sheets its properties change rapidly and material behaves more like graphite [10]. Graphene oxide is a one of graphene derivatives, obtained by chemical oxidation. The structure of GO consists of graphene layer with functional groups attached to the surface [11]. Number and type of oxygen groups like hydroxyl, epoxide and carboxyl groups determine the properties of graphene oxide [12]. Thanks to its reactive groups, GO can interact with polymer matrix and form stable colloidal emulsion in polar solvents [11,13]. It has been reported that GO promotes proliferation of various types of cells [1,14] and exhibits antibacterial activity [15]. The most common way of GO preparation is Hummers method [16] and its modifications. Graphite flakes are oxidized using $NaNO_3$ and $KMNO_4$ dissolved in concentrated H_2SO_4. Hummers method was improved by Marcano [17]. In the modified procedure, $NaNO_3$ was eliminated and mixture of H_2SO_4 and H_3PO_4 was introduced. This allowed to synthesize more oxidized and hydrophilic GO and eliminate production of toxic gases (NO_2, N_2O_4).

Reduced graphene oxide (rGO) can be synthesized by chemical, thermal or UV exposure reduction of GO. GO and rGO have different chemical and physical properties [18], rGO is less stable in solution [19] and shows electrical conductivity [20]. It was also reported that GO and rGO affect the cells in different ways [21,22]. Most common rGO synthesis method is chemical reduction of GO sheets using hydrazine (N_2H_4) [23]. However, hydrazine is highly toxic [24] and not suitable for biomedical applications. L-ascorbic acid is nontoxic and effectively reduces GO, hence it can be an alternative reducing agent to hydrazine [25,26].

Recently, modification of polymer matrix with GO and rGO becomes more and more popular due to their favorable mechanical properties, biocompatibility and the fact that both those nanofillers can potentially provide novel properties to the scaffold for tissue engineering. Chitosan is one of naturally occurring polymers with great biocompatibility [27] and biodegradability [28]. However, its applications are limited by low mechanical properties and necessity of cross-linking with e.g. chemical agents. It was reported that graphene derivatives like GO and rGO have positive influence on chitosan physical [29] and biological [13] properties, as well as degradation behaviour [30]. In this work we present simple and green method of GO synthesis (modified Marcano method) and reduction with L-ascorbic acid. Next we investigated the relation between type and content of nanoparticles and the morphology, structure, mechanical properties and degradation behavior of the chitosan-based composite films.

Materials and Methods

Materials

High molecular weight chitosan (M = 600 000 – 800 000 g/mol) with 90% deacetylated was purchased from Acros Organics, USA. Concentrated acetic acid and L-ascorbic acid were purchased from Avantor Performance Materials Poland S.A. Hydroxyapatite (HA) was purchased from Chema-Elektromet, Poland.

Graphene Oxide (GO) was prepared in the Institute of Electronic Materials Technology (ITME), Poland by modified Marcano method, as described previously in [31]. Briefly, oxidation of graphite was carried out by mixing graphite flakes with oxidant agent, potassium permanganate ($KMnO_4$) in the presence of sulfuric acid (H_2SO_4) and phosphoric acid (H_3PO_4). The mixture was kept for 4 hours under vigorous stirring. Next, perhydrol was added. Then the mixture was cooled down and washed with hydrochloric acid (HCl) aqueous solution and distilled water. Material was mechanically exfoliated to obtain flakes as thin as possible. The suspension was freeze-dried.

GO reduction was performed in the water solution of L-ascorbic acid (L-AA) and sodium hydroxide (NaOH). In typical experiment 300 mg of L-AA was added to 300 ml aqueous suspension of GO (0.01 mg/ml). Next, NaOH solution (1M) was dripped to adjust the pH to 9-10. In alkaline conditions GO sheets exhibit the best colloidal stability thanks to the electrostatic repulsion forces. The whole system was sonicated for 1 h, heated to 70°C and kept under vigorous stirring for 2 h. After the reduction, the material was centrifuged and washed with distilled water until the pH was neutral, followed by freeze-drying.

The chitosan/GO composite films were prepared by solution casting method. Known amount of chitosan was dissolved in 5% acetic acid solution and stirred overnight using magnetic stirrer, in ambient conditions. GO flakes were dispersed in 10 ml distilled water and homogenized in ultrasonic bath for 3 h. Next, GO dispersion was gradually added to the chitosan solution, followed by stirring and sonication. The mass content of GO was: 0, 0.5, 1.0, 1.5, 2.0 and 3.0%. Finally solutions were casted onto Teflon dishes and left at room temperature for 96 h. The composite with 1.5% (w/w) rGO content was prepared by adding appropriate amount of the previously prepared rGO to the chitosan solution. Also, chitosan/rGO/hydroxyapatite (HA) (6.0% w/w) composites were fabricated.

Methods

Morphology analysis

Microstructure of the composites was characterized by scanning electron microscopy (SEM) (Nova NanoSEM 200). To measure the pore diameter, the composites were freeze-dried and then cut into thin slices with a scalpel. As prepared porous samples were mounted onto holder and coated with conductive carbon layer prior to SEM analysis.

Structural analysis

The structural properties of the nanoparticles and composite films were investigated by X-ray diffraction (XRD) using X'Pert Pro diffractometer with Cu Kα X-ray sources (λ = 1.5406 Å) and attenuated total reflection Fourier-transform infrared spectroscopy (ATR-FTIR) using Bruker Tensor 27 equipment.

Mechanical properties

Tensile test of the composite films was performed on universal mechanical tester (Zwick 1435). The samples were cut into strips with a dimension of 5 mm x 30 mm; testing speed was 1 mm/min.

Wettability

The contact angle of composite films was measured by sessile drop method (Krüss Drop Shape Analyzer). Ten drops of deionized water were tested for each samples and the average value was calculated.

***In vitro* degradation**

In vitro degradation test of the composites was carried out in distilled water, phosphate buffered saline (PBS), and Ringer's solution. The samples were incubated for 2 months, at 37°C.

Results and Discussions

Characterization of GO and rGO powders

GO, synthesized by oxidation and exfoliation of graphite flakes by modified Marcano method was characterized by ATR and XRD. The FTIR-ATR spectra of GO presented in FIG. 1 shows five main peaks which can be assigned to: O-H groups (3404 cm^{-1}), C=O stretching vibrations of carboxylic groups (1738 cm^{-1}), C=C stretching of the sp^2 network (1662 cm^{-1}), C-O groups in C-OH (1370 cm^{-1}), C-O stretching vibration of C-O-C (1113 cm^{-1}). In the case of rGO, intensity of the peaks decreased dramatically. It confirmed that the oxygen groups can be removed in reduction process using L-ascorbic acid. X-ray diffraction pattern (FIG. 2) of GO shows sharp peak at 11.51° (peak is marked with a black square; rest of the peaks in the pattern come from excipient used for XRD analysis), which completely disappeared after GO reduction and a new wide peak showed up at 22.83°.

The interlayer spacing of the GO powder at ~0.77 nm decreased to ~0.39 nm what is the effect of removing oxygen functional groups. During the reduction, the functional groups are removed from the graphene sheets by reacting with the hydrogen atoms from the L-ascorbic acid, and water is produced. Nucleophilic attack and thermal reduction restore C=C bonds. Alkaline conditions ensure electrostatic repulsion of graphene sheets, which hinders π-π stacking between sheets and prevents agglomeration [26].

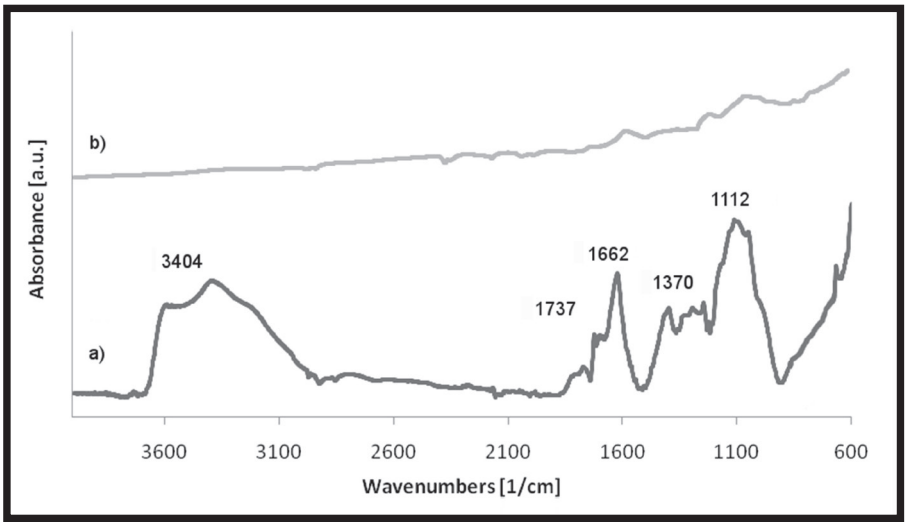

FIG. 1. ATR spectra of: a) GO, b) rGO.

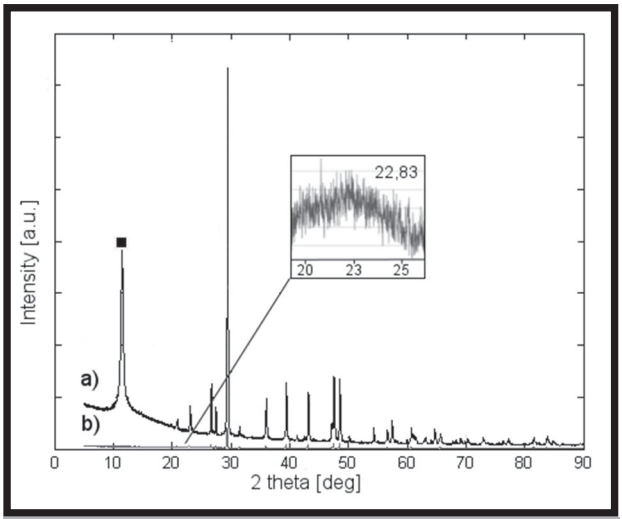

FIG. 2. X-ray diffraction of: a) GO, b) rGO.

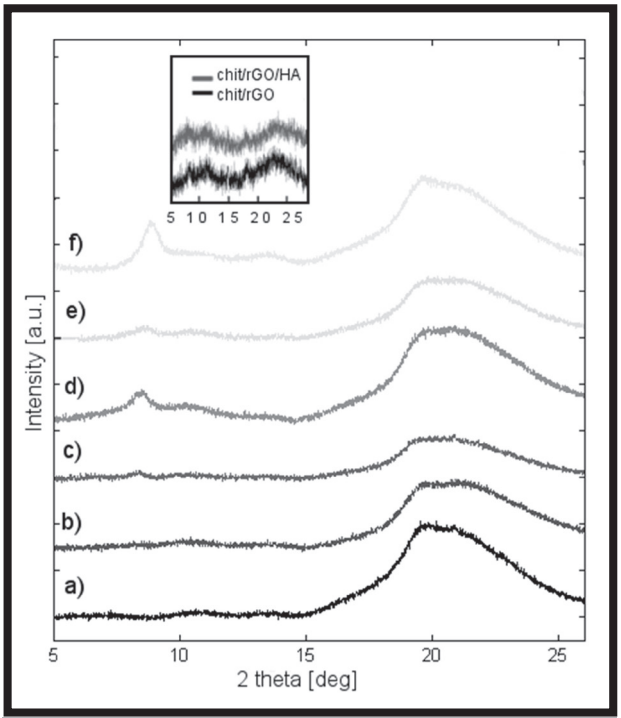

FIG. 3. X-ray diffraction patterns of chitosan: a) pure, b) 0.5% GO, c) 1.0% GO, d) 1.5% GO, e) 2.0% GO, f) 3.0% of GO and films with 1.5% rGO and 6% HA.

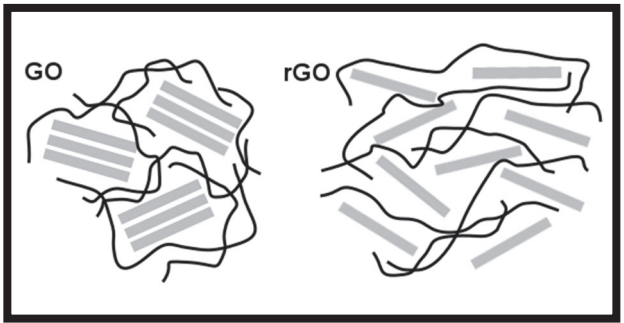

FIG. 4. Schematic representation of behaviour of GO and exfoliated rGO sheets in polymer matrix.

Characterization of the nanocomposites

Chitosan films containing 0.5%, 1.0%, 1.5%, 2.0% and 3.0% of GO were prepared by mixing dispersion of the nanofillers with the polymer solution. Nanocomposites with 1.5% of rGO and 6.0% of HA were also fabricated. Interaction between matrix and fillers, dispersion of graphene derivatives and chitosan crystallinity were analyzed by SEM and XRD.

XRD patterns of chitosan films modified with GO are shown in FIG. 3. Broad peak at 20° is referred to the amorphous structure of pristine chitosan. Weak diffraction peak for the nanocomposites with 1.5%, 2.0% and 3.0% GO can be also seen at 8° and corresponds to the crystalline phase formed as a result of graphene oxide addition. Due to the low content of the nanofiller and good dispersion in the matrix, peaks characteristic for GO are not detected in the composites. The degree of chitosan crystallinity can be calculated on the basis of the peak area according to the formula:

$$x_c = \frac{I_c}{I_c + I_a} \qquad (1)$$

Where I_c is an area of peak corresponding to the crystalline structure and I_a is a peak area of amorphous phase. The crystallinity degree of the nanocomposites was 2.5%, 4.6%, 4.3% and 8.6% for chitosan with 1.0%, 1.5%, 2.0% and 3.0% of GO, respectively. The structure of the pure chitosan and the nanocomposites with 0.5%, 1.0% of GO content was amorphous. The presence of GO in the casted chitosan solution promoted the crystallization process by a nucleation effect.

Nanocomposites with rGO were prepared with the simultaneous reduction of graphene oxide under alkaline conditions that caused electrostatic repulsion of the GO sheets. The volume fraction of the exfoliated, individual rGO sheets dispersed in the polymer matrix were higher than GO, despite the same mass content, and caused the self-organization of the composite (FIG. 4). XRD patterns of the film with rGO present very weak, broad peaks (FIG. 3). Reduction of GO increased the surface area and volume of the nanofiller in the matrix. Chitosan chains attached to the surface of the rGO sheets due to the physical interaction.

SEM analysis of the surface morphology clearly showed differences between composites with GO and rGO (FIG. 5). Surface of the pristine chitosan was homogeneous and smooth (FIG. 5a). In the case of the films with GO, the surface roughness increased with the mass content of the filler (FIG. 5b, c, d). However, the surfaces were still quite smooth, which was due to the low content of GO and low exfoliation of GO sheets. On the other hand, surfaces of the films with rGO were rough and a lot of rGO sheets were visible (FIG. 5e). As shown in FIG. 5f, homogenously dispersed HA particles, densely planted surface of the film, further increasing roughness what can potentially improve cells adhesion.

Samples after freeze-drying were cut into slices to analyze the shape and pore size under SEM as shown in FIG. 6. The pore diameter of pristine chitosan was in the range of 100-150 μm. The pores formed a dense network of interconnected channels. Introduction of GO reduced the pore diameter but did not affect their shape. Pore walls remained thin and smooth (FIG. 6a, b). Significant differences are seen for the samples with rGO. Pores are bigger, with diameter around 200 μm (FIG. 6.c, e) and their walls are thick and rough (FIG. 6d, f). During the manufacture of the composites with the simultaneous reduction of GO, chitosan chains attached to the exfoliated rGO sheets, connecting them together and forming thick wall with rough surface.

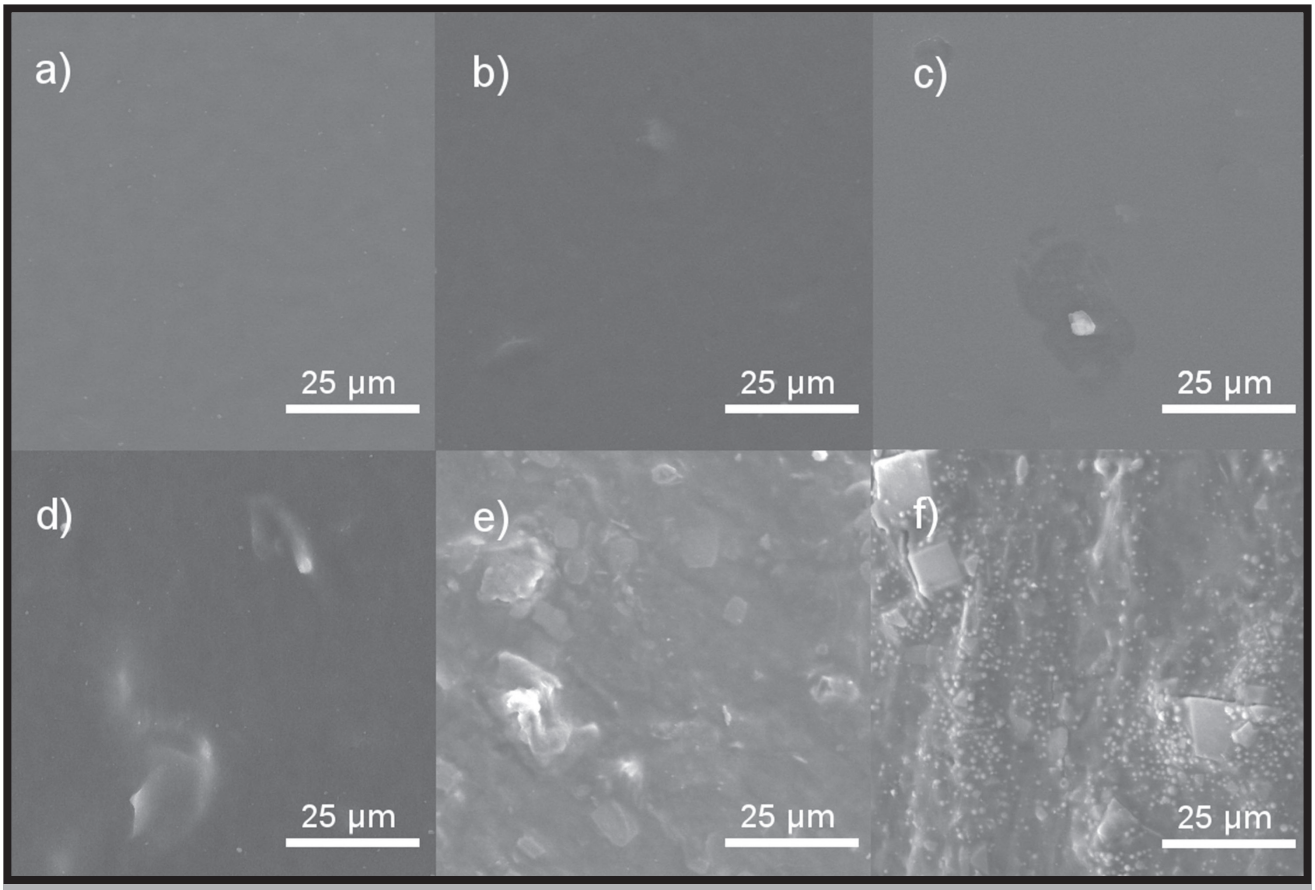

FIG. 5. SEM images of chitosan film microstructure: a) pure, b) with 0.5% GO, c) 1.5% GO, d) 3.0% GO, e) 1.5% rGO, f) 1.5% rGO and 6.0% HA.

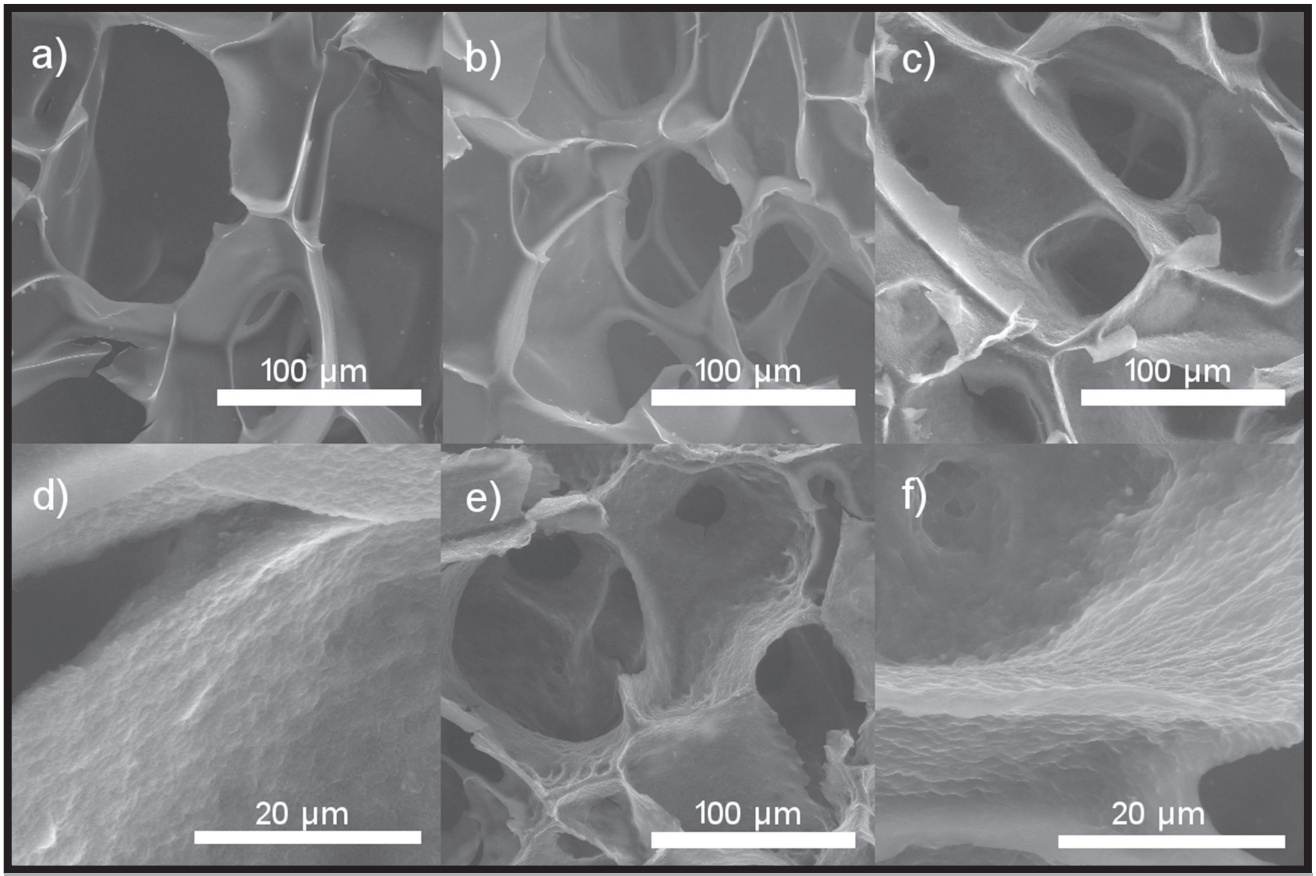

FIG. 6. SEM images of a) chitosan b) chitosan/1.5% GO, c,d) chitosan/1.5% rGO, e,f)) chitosan/1.5% rGO/6.0% HA.

TABLE 1. Properties of chitosan and nanocomposites modified with GO, rGO and HA (mean ± SD).

Sample	Average pore diameter [μm]	Contact angle [deg]	Young's modulus [MPa]
Chitosan	117 ± 34	110 ± 22	2035 ± 156
Chitosan/0.5% GO	86 ± 22	106 ± 2	1851 ± 213
Chitosan/1.0% GO	68 ± 16	91 ± 2	2296 ± 391
Chitosan/1.5% GO	68 ± 19	103 ± 4	2749 ± 253
Chitosan/2.0% GO	60 ± 14	96 ± 2	2341 ± 58
Chitosan/3.0% GO	60 ± 15	85 ± 3	1369 ± 17
Chitosan/1.5% rGO	184 ± 29	75 ± 4	443 ± 99
Chitosan/1.5% rGO/6.0% HA	204 ± 25	65 ± 4	803 ± 76

TABLE 2. Weight loss of composites with rGO and HA (mean ± SD).

Solution	Weight loss [%]			
	Chitosan/1.5% rGO		Chitosan/1.5% rGO/6.0% HA	
	1 month	2 month	1 month	2 month
Distilled water	55 ± 3	58 ± 3	53 ± 2	56 ± 3
PBS	47 ± 2	53 ± 3	45 ± 2	52 ± 3
Ringer	42 ± 2	48 ± 2	46 ± 2	57 ± 3

The average pore diameter for all types of the scaffolds is summarized in TABLE 1. The scaffold for bone regeneration must be highly porous and the pores should create a network to allow cell infiltration and diffusion of nutrients, waste and oxygen. Another advantage is the roughness of the walls, which can facilitate cells adhesion. The pore diameter should not be less than about 200 μm [32]. From this perspective, the composite scaffolds with rGO, and rGO with HA were found as most suitable for application in tissue engineering.

Another important factor that determines the attachment of the cells to the scaffold's surface is appropriate wettability. High contact angle of the chitosan is due to its hydrophobic nature. When the content of GO increases, the contact angle decreases (TABLE 1), improving the hydrophilicity. This is an effect of the increased surface roughness and the presence of hydrophilic functional groups on the GO sheets. However, the addition of 1.5% GO reduced the contact angle by only 7°. The surface of the film was still smooth and nanofillers were rarely seen. The greatest improvement in wettability, resulting in fully hydrophilic character, was observed for composites with rGO. This is due to different process of composite formation. Exfoliated, well-visible under SEM rGO sheets, surrounded by chitosan, created a unique, microscale roughness features on the film surface. In addition, there were many well-dispersed spherical particles on the surface of the film containing HA. This led to a decrease of the water contact angle from 117° to 75° and 65° for chitosan/rGO and chitosan/rGO/HA, respectively.

The mechanical properties of the films were characterized by the uniaxial tensile test. Generally, the composites with GO were tough and fragile. The Young's modulus increased with the nanofiller content up to 2.0%, as shown in TABLE 1. The best enhancement effect was obtained for the composite with 1.5% GO, in which the Young's modulus increased by 35%. Improvement in the mechanical properties can be attributed to the high surface area of the GO sheets and their good dispersion in the polymer matrix. The decrease of the mechanical properties of 3.0% for GO composite can be related to the agglomeration of the filler. Composites modified with rGO behaved differently. They were soft and easy to bend without cracking but at the same time, only small force was needed to break them. The exfoliated, oriented rGO sheets with strong π-π interactions were joined by chitosan chains during the composite fabrication with the simultaneous reduction of GO by L-ascorbic acid. Chemical cross-linkers were not used to create bonds between polymer chains. However, degradation behaviour of the composites showed that rGO could work as physical cross-linking agent and stabilized polymer network. Films containing GO dissolved after one day of incubation at 37°C, thus it can be concluded that the chemical bonds between chitosan and functional groups attached to the nanosheets surface were not created. Composites with rGO showed good stability in all analysed liquids. Weight loss after 1 and 2 months is shown in TABLE 2. Degradation behavior of all the samples was similar. The first stage was faster, the weight of the samples reduced by half; however the samples kept their shape and did not break apart. The second stage was slower and the weight loss for each sample increased by only few percent. There were no significant differences between the composite with rGO only and the composite with rGO and HA.

Conclusions

We presented a simple method of fabrication of chitosan composites with the simultaneous reduction of GO with a non-toxic reducing agent, L-ascorbic acid. Chitosan properties like surface wettability, stability during degradation at the human body temperature or pore structure were improved thanks to the rGO addition. Due to the exfoliation of the nanosheets and their uniform distribution, hydrogels exhibited properties potentially useful in tissue engineering. Further tests, including biocompatibility and antibacterial activity evaluation are necessary.

Acknowledgments

Joanna Jagiełło and Dr. Ludwika Lipińska from the Institute of Electronic Materials Technology (ITME) in Warsaw are gratefully acknowledged for providing graphene oxide. This research was financed by the grant No 15.11.160.019 (Faculty of Materials Science and Ceramics, AGH UST). The National Centre for Research and Development, Poland is gratefully acknowledged for providing financial support under STRATEGMED program: grant No. STRATEGMED3/303570/7/NCBR/201.

References

[1] Shin, S. R. et al.: Graphene-based materials for tissue engineering. Advanced Drug Delivery Reviews 105 (2016) 255-274.
[2] Lin, J., Chen, X. & Huang, P.: Graphene-based nanomaterials for bioimaging. Advanced Drug Delivery Reviews 105 (2016) 242-254.
[3] Justino C.I.L., Gomes A.R., Freitas A.C., Duarte A.C., Rocha-Santos T.A.P.: Graphene based sensors and biosensors. TrAC Trends in Analytical Chemistry 91 (2017) 53-66.
[4] Zhang, Q. et al.: Advanced review of graphene-based nanomaterials in drug delivery systems: Synthesis, modification, toxicity and application. Materials Science and Engineering: C 77 (2017) 1363-1375.
[5] Georgantzinos S.K., Giannopoulos G.I., Fatsis A., Vlachakis N.V.: Analytical expressions for electrostatics of graphene structures. Physica E: Low-dimensional Systems and Nanostructures 84 (2016) 27-36.
[6] Lee C., Wei X., Kysar J.W., Hone J.: Measurement of the Elastic Properties and Intrinsic Strength of Monolayer Graphene. Science 321 (2008) 385-388.
[7] Wu Z.-S. et al.: Synthesis of Graphene Sheets with High Electrical Conductivity and Good Thermal Stability by Hydrogen Arc Discharge Exfoliation. ACS Nano 3 (2009) 411-417.
[8] Balandin, A. A. et al.: Superior Thermal Conductivity of Single-Layer Graphene. Nano Letters 8 (2008) 902-907.
[9] Sharon M., Sharon M.: Graphene: an introduction to the fundamentals and industrial applications. Wiley (2015)
[10] Geim A.K., Novoselov K.S.: The rise of graphene. Nature Materials 6 (2007) 183-191.
[11] Dreyer D.R., Park S., Bielawski C. W., Ruoff R.S.: The chemistry of graphene oxide. Chem. Soc. Rev. 39 (2010) 228-240.
[12] Yan J.-A., Chou M.Y.: Oxidation functional groups on graphene: Structural and electronic properties. Physical Review B 82 (2010).
[13] Pandele A.M. et al.: Preparation and in vitro, bulk, and surface investigation of chitosan/graphene oxide composite films. Polymer Composites 34 (2013) 2116-2124.
[14] Kim T.-H., Lee T., El-Said W., Choi J.-W.: Graphene-Based Materials for Stem Cell Applications. Materials 8 (2015) 8674-8690.
[15] Liu S. et al.: Antibacterial Activity of Graphite, Graphite Oxide, Graphene Oxide, and Reduced Graphene Oxide: Membrane and Oxidative Stress. ACS Nano 5 (2011) 6971-6980.
[16] Hummers W.S., Offeman R.E.: Preparation of Graphitic Oxide. Journal of the American Chemical Society 80 (1958) 1339-1339.
[17] Marcano D.C. et al.: Improved Synthesis of Graphene Oxide. ACS Nano 4 (2010) 4806-4814.
[18] Pei S., Cheng H.-M.: The reduction of graphene oxide. Carbon 50 (2012) 3210-3228.
[19] Konios D., Stylianakis M.M., Stratakis E., Kymakis E.: Dispersion behaviour of graphene oxide and reduced graphene oxide. Journal of Colloid and Interface Science 430 (2014) 108-112.
[20] Li Z.J., Yang B.C., Zhang S.R., Zhao C.M.: Graphene oxide with improved electrical conductivity for supercapacitor electrodes. Applied Surface Science 258 (2012) 3726-3731.
[21] Kang Y. et al.: Graphene oxide and reduced graphene oxide induced neural pheochromocytoma-derived PC12 cell lines apoptosis and cell cycle alterations via the ERK signaling pathways. International Journal of Nanomedicine 12 (2017) 5501-5510.
[22] Katsumiti A., Tomovska R., Cajaraville M.P.: Intracellular localization and toxicity of graphene oxide and reduced graphene oxide nanoplatelets to mussel hemocytes in vitro. Aquatic Toxicology 188 (2017) 138-147.
[23] Park S. et al.: Hydrazine-reduction of graphite- and graphene oxide. Carbon 49 (2011) 3019-3023.
[24] Guldberg Klenø T. et al.: Mechanisms of hydrazine toxicity in rat liver investigated by proteomics and multivariate data analysis. PROTEOMICS 4 (2004) 868-880.
[25] Zhang J. et al.: Reduction of graphene oxide via L-ascorbic acid. Chem. Commun. 46 (2010) 1112-1114.
[26] Xu C. et al.: Fabrication and Characteristics of Reduced Graphene Oxide Produced with Different Green Reductants. PLOS ONE 10, e0144842 (2015).
[27] Croisier F., Jérôme C.: Chitosan-based biomaterials for tissue engineering. European Polymer Journal 49 (2013) 780-792.
[28] Landriscina A., Rosen J., Friedman A.J.: Biodegradable chitosan nanoparticles in drug delivery for infectious disease. Nanomedicine 10 (2015) 1609-1619.
[29] Yadav S.K. et al.: Mechanically Robust, Electrically Conductive Biocomposite Films Using Antimicrobial Chitosan-Functionalized Graphenes. Particle & Particle Systems Characterization 30 (2013) 721-727.
[30] Depan D., Shah J.S., Misra R.D.K.: Degradation mechanism and increased stability of chitosan-based hybrid scaffolds cross-linked with nanostructured carbon: Process–structure–functional property relationship. Polymer Degradation and Stability 98 (2013) 2331-2339.
[31] Jaworski S., Sawosz E., Kutwin M., et al.: In vitro and in vivo effects of graphene oxide and reduced graphene oxide on glioblastoma. International Journal of Nanomedicine 10 (2015) 1585-1596.
[32] Levengood S.L., Zgang M.: Chitosan-based scaffolds for bone tissue engineering. Journal of Materials Chemistry B 2(21) (2014) 3161-3184.

KOFEINA JAKO CZYNNIK MODYFIKUJĄCY HYDROŻELE AKRYLOWE

Bożena Tyliszczak[1], Sonia Kudłacik-Kramarczyk[2]*, Anna Drabczyk[2]

[1] Katedra Chemii i Technologii Polimerów, Politechnika Krakowska im. Tadeusza Kościuszki, ul. Warszawska 24, 31-155 Kraków
[2] Instytut Chemii i Technologii Nieorganicznej, Politechnika Krakowska im. Tadeusza Kościuszki, ul. Warszawska 24, 31-155 Kraków
*e-mail: skudlacik@chemia.pk.edu.pl

Streszczenie

Hydrożele są materiałami zbudowanymi z łańcuchów polimerowych, które tworzą trójwymiarową i usieciowaną strukturę. Mają one bardzo dużą zdolność do pochłaniania wody, stąd też bardzo często są nazywane superabsorbentami. Inne cechy charakteryzujące hydrożele to elastyczność oraz nietoksyczność. Poprzez swoje właściwości hydrożele są często stosowane w inżynierii tkankowej, układach dostarczania leku czy w opatrunkach hydrożelowych. Celem pracy była ocena wpływu modyfikacji matrycy polimerowej kofeiną na właściwości i strukturę hydrożeli, natomiast zakres pracy obejmował syntezę i modyfikację matrycy polimerowej oraz badania inkubacyjne in vitro, spektroskopowe i fizykochemiczne. W pracy zostały przeprowadzone i omówione badania hydrożeli modyfikowanych różną zawartością kofeiny. Hydrożele zostały poddane badaniom sprawdzającym ich zdolność absorpcyjną w roztworach składem przypominającym płyny ustrojowe organizmu ludzkiego. Przeprowadzono również badania zachowania się hydrożeli w płynach ustrojowych jakimi były woda destylowana, płyn Ringera i sztuczna ślina. Na podstawie przeprowadzonych badań można wstępnie stwierdzić, że otrzymane materiały nie powodują zmian pH roztworów, w których są inkubowane. Ponadto, uwalniają one wprowadzoną do ich struktury kofeinę. Tak otrzymane wyniki, pozwalają stwierdzić, że materiał otrzymany przy pomocy fotopolimeryzacji na bazie kwasu akrylowego może znaleźć zastosowanie w takich dziedzinach jak medycyna czy kosmetologia.

Słowa kluczowe: *hydrożele, kofeina, badania inkubacyjne, spektroskopia FT-IR*

[Inżynieria Biomateriałów 142 (2017) 17-24]

Wprowadzenie

Hydrożele są materiałami polimerowymi, które cieszą się w ostatnich latach bardzo dużą popularnością. Powodem tego są ich specyficzne cechy, między innymi elastyczność, możliwość bardzo szybkiego pochłaniania wody i innych roztworów w sposób odwracalny, bardzo duża aktywność biologiczna z płynami ustrojowymi organizmu ludzkiego oraz biodegradowalność [1-3]. Dzięki swoim unikalnym cechom hydrożele znalazły szerokie zastosowanie w wielu dziedzinach życia takich jak farmacja, rolnictwo, medycyna czy inżynieria tkankowa [4-6].

CAFFEINE AS A MODIFYING AGENT IN ACRYLIC HYDROGELS

Bożena Tyliszczak[1], Sonia Kudłacik-Kramarczyk[2]*, Anna Drabczyk[2]

[1] Department of Chemistry and Technology of Polymers, Cracow University of Technology, Warszawska 24, 31-155 Krakow, Poland
[2] Institute of Inorganic Chemistry and Technology, Cracow University of Technology, Warszawska 24, 31-155 Krakow, Poland
*e-mail: skudlacik@chemia.pk.edu.pl

Abstract

Hydrogels are materials created by polymer chains, that form a three-dimensional and crosslinked structure. These polymers are characterized by a very high sorption capacity, therefore they belong to the group of substances known as superabsorbents. Due to their properties hydrogels are often used in tissue engineering, drug delivery systems and as components of modern wound dressings. The aim of the study is to evaluate the effect of introduction of caffeine into the polymer matrix on the properties and structure of hydrogels. The scope of work included the synthesis and modification of the polymer matrix as well as studies on such prepared materials. Research involved in vitro incubation, spectroscopic analysis, studies on degradation and characterization of other physico-chemical properties. In this article series of hydrogels based on acrylic acid and modified with different amount of caffeine have been synthesized. The sorption capacity of obtained hydrogels in the liquids with compositions similar to the human body fluids has been tested. The stability of synthesized materials in simulated body fluids such as Ringer's solution and artificial saliva has also been analysed. Based on conducted research it can be said that prepared materials do not change pH value of a liquid in which they are immersed. What is more, they are able to release entrapped caffeine. On the basis of such results it can be concluded that proposed acrylic acid based materials obtained by means of photopolymerization can be used in such areas as medicine or cosmetology.

Keywords: *hydrogels, caffeine, incubation studies, FT-IR spectroscopy*

[Engineering of Biomaterials 142 (2017) 17-24]

Introduction

Hydrogels are polymeric materials which become more and more popular in recent years. The reason for this are their specific features such as flexibility, ability to absorb water and other liquids quickly and in a reversible manner, a very high biological activity in contact with the human body fluids and often biodegradability [1-3]. Due to their unique features hydrogels are widely used in many areas such as pharmacy, agriculture, medicine and tissue engineering [4-6].

Interesującą cechą materiałów hydrożelowych jest możliwość ich modyfikacji poprzez wprowadzenie do matrycy hydrożelowej związków zarówno pochodzenia naturalnego, jak i syntetycznego. Taki dodatek może wpłynąć na właściwości fizykochemiczne hydrożeli polimerowych, tj. ich zdolności sorpcyjne czy również właściwości mechaniczne. Należy jednak zaznaczyć, że wprowadzenie dodatkowej substancji do wnętrza materiału hydrożelowego niekoniecznie zmienia właściwości chemiczne, a jedynie wpływa na zwiększenie spektrum jego potencjalnych zastosowań. Rolę dodatku mogą pełnić różnego rodzaju substancje aktywne takie jak np. kofeina, ale również ekstrakty roślinne (np. ekstrakt z szałwii czy rumianku), czy różne nanomateriały [7-9].

Celem pracy było zsyntezowanie hydrożelu, w którym matryca polimerowa została zmodyfikowana kofeiną. Połączenie hydrożelu z kofeiną wydaje się być bardzo ciekawym rozwiązaniem, który może znaleźć dość szerokie zastosowanie w medycynie bądź farmacji, ze względu na właściwości zarówno hydrożeli, jak i kofeiny. Kofeina jest związkiem, który można pozyskiwać z nasion kawy czy herbaty, a wyekstrahowana może być używana do wielu celów leczniczych, między innymi do leczenia bólu głowy czy nadwagi [10-12]. Kofeina jest materiałem szeroko stosowanym w kosmetyce np. do zmniejszania cieni pod oczami, czy do walki z cellulitem. Ponieważ, kofeina jest często spożywana głównie w postaci kawy, leków przeciwbólowych czy Coca-Coli, to należy brać pod uwagę jej różnorodne spektrum działania i zwracać uwagę na ilość, w jakiej występuje w przyjmowanych produktach. Może ona wywierać również negatywny wpływ na organizm ludzki przy przekroczeniu dopuszczalnej dawki [13-15].

Materiały i Metody

Materiały

Kwas akrylowy (AA), wodorotlenek potasu (KOH) i kofeina zostały pozyskane z firmy POCh Gliwice, Polska. Natomiast, diakrylan poli(glikolu etylenowego) (DAPEG Mw = 256) oraz tlenek fenylobis(2,4,6-trimetylobenzoilo) fosfiny zakupiono w Sigma Aldrich. Wszystkie substancje użyte do badań oraz syntezy były czystości analitycznej.

Synteza materiałów hydrożelowych

Przygotowanie opisywanych materiałów poprzedzono serią syntez mającą na celu dobór ilości fotoinicjatora oraz czynnika sieciującego. Brano pod uwagę stopień usieciowania otrzymanych materiałów, jak również ich elastyczność.

W celu wykonania hydrożelu należy zobojętnić 45 ml kwasu akrylowego 50 ml 40% roztworu KOH. Ze względu na charakter egzotermiczny reakcji była ona prowadzona w medium chłodzącym, którym była woda o temp. 10°C. Po osiągnięciu temperatury pokojowej (20°C) pobrano 15 ml mieszaniny i w przeliczeniu na czysty kwas akrylowy zawarty w 15 ml mieszaniny dodano wyliczoną ilość kofeiny w ilości 0%, 1%, 3%, 5%, 7% masowych oraz po 1 ml fotoinicjatora (2 g tlenku fenylobis(2,4,6-trimetylobenzoilo)fosfiny + 10 ml kwasu akrylowego) i 1 ml czynnika sieciującego (DAPEG 256). Synteza hydrożelu prowadzona była pod lampą UV (1 min).

Otrzymane materiały wysuszono w temperaturze pokojowej, a następnie poddawano je działaniu gorącej pary wodnej w celu sterylizacji.

The interesting feature of hydrogel materials is the ability of their modification by introduction of natural and synthetic compounds into the hydrogel matrix. Such addition may affect the physicochemical properties of hydrogels including their sorption capacity or mechanical properties. However, it should be noted that the introduction of an additional substance into the interior of such material may not affect its chemical properties, but only increase a range of its potential applications. The role of the additive can be played by various active substances such as caffeine, plant extracts (e.g. sage or camomile extract) or nanomaterials [7-9].

The main purpose of this study was to obtain a hydrogel, wherein its matrix has been modified with caffeine. The combination of the hydrogel with this substance seems to be very promising for the use in medicine or pharmacy, due to the properties of both the hydrogel and caffeine. The additive to the polymer matrix is a compound that can be obtained from the seeds of coffee or tea leaves. The extracted compound can be used for many medical purposes such as the treatment of headache or overweight [10-12]. Caffeine is a material widely used in cosmetics, for example it is applied for cellulite reducing. This active substance is mainly consumed in the form of coffee, analgesic, or as a component of energy drinks. Therefore, the diverse range of its effects should be taken into account and attention should be paid to the amount in which it appears in consumed products. Caffeine can also have a negative impact on the human body after exceeding the permissible dose [13-15].

Materials and Methods

Materials

Acrylic acid (AA), potassium hydroxide (KOH) and caffeine were bought from Avantor Performance Materials Poland S.A. (formerly POCh S.A.). Poly(ethylene glycol) diacrylate (PEGDA) (M = 256) and phenylbis (2,4,6-trimethylbenzoyl)phosphine oxide were received from Sigma Aldrich. All these substances were applied without further purification.

Preparation of hydrogels

Preparation of the described materials was preceded by a series of syntheses conducted in order to select the suitable amounts of photoinitiator and crosslinking agent. The crosslinking degree of obtained materials as well as their flexibility were considered during the selection of the appropriate amounts of the mentioned reagents.

In order to synthesize hydrogels 45 ml of acrylic acid was neutralized using 50 ml of 40% KOH solution. The obtained mixture was kept in a cooling medium (water, 10°C) due to the exothermic character of the reaction.

After reaching a room temperature (20°C) 15 ml of the mixture was added to a calculated amount of a caffeine (in a content of 0%, 1%, 3%, 5%, 7% by weight based on the amount of acrylic acid in a mixture). In the next step 1 ml of a photoinitiator solution (2 g phenylbis(2,4,6-trimethylbenzoyl)phosphine oxide in 10 ml of acrylic acid) and 1 ml of crosslinker (PEGDA 256) were added and the obtained mixture was poured into a Petri dish and treated with UV radiation for 1 min.

Prepared materials were dried at room temperature and subsequently treated with the hot steam sterilization.

Badanie zdolności absorpcyjnych

Zdolność absorpcyjną badano w roztworach 0,9% NaCl, 0,9% $MgCl_2$, wodzie destylowanej, płynie Ringera i sztucznej ślinie. Suchą próbkę o masie zawierającej się pomiędzy 0,70 a 1 g umieszczano w 50 ml roztworu na czas 1 h, a następnie ważono mokry hydrożel i określano stopień pęcznienia. Stopień pęcznienia został obliczony na podstawie wzoru 1.

$$Q = \frac{w - w_0}{w_0} \qquad (1)$$

gdzie: *w* - masa próbki po spęcznieniu, w_0 - masa próbki przed spęcznieniem

Badanie powtórzono 3-krotnie dla każdej kompozycji, a przedstawione wyniki stanowią wartość średnią z uzyskanych wyników.

Badanie inkubacyjne

Badania inkubacyjne przeprowadzono w wodzie destylowanej (pH = 6,6), płynie Ringera (pH = 6,4) i sztucznej ślinie (pH = 5,75). Próbki o masie 1 g umieszczono w pojemnikach szczelnie zamkniętych na okres 10 tyg. w wodzie destylowanej i płynie Ringera oraz na 4 tyg. w sztucznej ślinie i co 7 dni mierzono pH. Badanie powtórzono 3-krotnie dla każdej kompozycji, a przedstawione wyniki stanowią wartość średnią z uzyskanych wyników.

Badanie spektroskopowe

Badania za pomocą spektroskopii fourierowskiej w podczerwieni metodą osłabionego całkowitego odbicia FTIR-ATR przeprowadzone były na wysuszonych hydrożelach po zakończeniu badania inkubacyjnego. Każdy hydrożel został przebadany na spektroskopie SPECTRUM 65 Perkin Elmer, który posiada kryształ z selenku cynku.

Wszystkie badania były przeprowadzane w temperaturze pokojowej i pod ciśnieniem atmosferycznym.

Wyniki i dyskusja

Badanie zdolności absorpcyjnej

Badanie pęcznienia materiałów hydrożelowych przez różny okres czasu jest często zależne od ich przeznaczenia. W związku z tym, że materiały będące przedmiotem niniejszej pracy były modyfikowane kofeiną, to ich głównym przeznaczeniem może być przemysł kosmetologiczny. Dlatego też badanie pęcznienia prowadzone było w czasie 1 h, gdyż np. płatki kosmetyczne pod oczy niwelujące obrzęki, stosuje się przez około 20-30 min. Warto również wspomnieć, że pęcznienie zależy w dużej mierze od zastosowanego czynnika sieciującego. Im więcej łańcuchów poprzecznych w sieci polimerowej, tym mniejsza zdolność do pęcznienia badanych materiałów. Jednak jak wspomniano na początku, naszym głównym celem było sprawdzenie pęcznienia w krótkim czasie. Na RYS. 1 przedstawiono wyniki opisujące zdolność pęcznienia otrzymanych materiałów hydrożelowych w różnych płynach.

Największa absorpcja roztworu przez hydrożele miała miejsce w wodzie destylowanej, natomiast najmniejsza w $MgCl_2$. W roztworze NaCl zdolności absorpcyjne hydrożeli są zdecydowanie mniejsze niż w wodzie, ponieważ dochodzi do wymiany pomiędzy jonami H^+ i Na^+. Jony te wpływają na zmniejszenie charakteru hydrofilowego grupy karboksylowej, poprzez reakcję zobojętnienia, co przyczynia się bezpośrednio do zmniejszenia chłonności w tym roztworze w porównaniu do wody destylowanej. W $MgCl_2$ występują kationy dwuwartościowe magnezu, które powodują znaczne zwiększenie stopnia usieciowania układu, który wpływa na zmniejszenie chłonności tego roztworu przez hydrożel.

Measurements of swelling ability

The absorption capacity was determined in the following liquids: 0.9% NaCl, 0.9% $MgCl_2$, distilled water, Ringer's solution and artificial saliva. The dry sample of a weight between 0.7 and 1 g was placed in 50 ml of above listed liquids for 1 h and after this time a wet hydrogel was weighed. The final step was the calculation of swelling ratio using the formula (1):

$$Q = \frac{w - w_0}{w_0} \qquad (1)$$

where: *w* was the weight of a sample after swelling, w_0 was the weight of dry hydrogel.

Measurements were repeated 3 times for each composition, and the presented results are the average of the obtained values.

Incubation studies

Incubation studies were carried out in distilled water (pH = 6.6), Ringer's solution (pH = 6.4) and artificial saliva (pH = 5.75) at 37°C. The samples weighing 1 g were placed in sealed vessels for a period of 10 weeks in the case of distilled water and Ringer's solution and for 4 weeks in the case of artificial saliva. pH of the liquids was measured every 7 days. Measurements were repeated 3 times for each sample. Presented results are the average of received values.

FT-IR spectroscopy

Attenuated total reflection Fourier transform infrared (ATR-FTIR) spectroscopy was performed using SPECTRUM 65 Perkin Elmer, zinc selenide was used as a crystal. Studies were conducted using hydrogels before and after incubation. All samples were thoroughly dried before the analysis. All tests were performed at room temperature under atmospheric pressure.

Results and Discussion

Swelling studies

Swelling studies conducted at different time intervals are usually dependent on potential applications of the tested materials. Due to the fact, that our hydrogels have been modified with caffeine, their main application involved cosmetic industry. Therefore, studies on sorption capacity of prepared hydrogels were carried out for 1 h, because, for example cosmetic flakes reducing swelling around eyes are applied for about 20-30 min. However, it should be mentioned that swelling process depends on many factors including type and amount of crosslinking agent used during the polymerization reaction. More crosslinks between polymer chains results in lower swelling ability of the tested hydrogels. Furthermore, as it was previously mentioned, our main purpose was to determine swelling ability of prepared materials in a short time period (such as 1 h). In FIG. 1 results of swelling degree of obtained hydrogels in selected fluids are shown.

The highest absorption of fluid was observed in the case of hydrogels immersed in distilled water, and the lowest in the case of $MgCl_2$. In the case of NaCl swelling capacity of hydrogels was significantly lower than in distilled water. It is caused by ion exchange between H^+ and Na^+ that takes place in the solution after immersion of the hydrogel sample. This ion exchange causes the reduction of the hydrophilic nature of the carboxyl group, which contributes directly to a decrease in the absorption potential of this solution in comparison with distilled water. In the $MgCl_2$ solution bivalent magnesium ions are present what results in a significant increase in the crosslinking degree. It causes the reduction of swelling capacity of the tested sample.

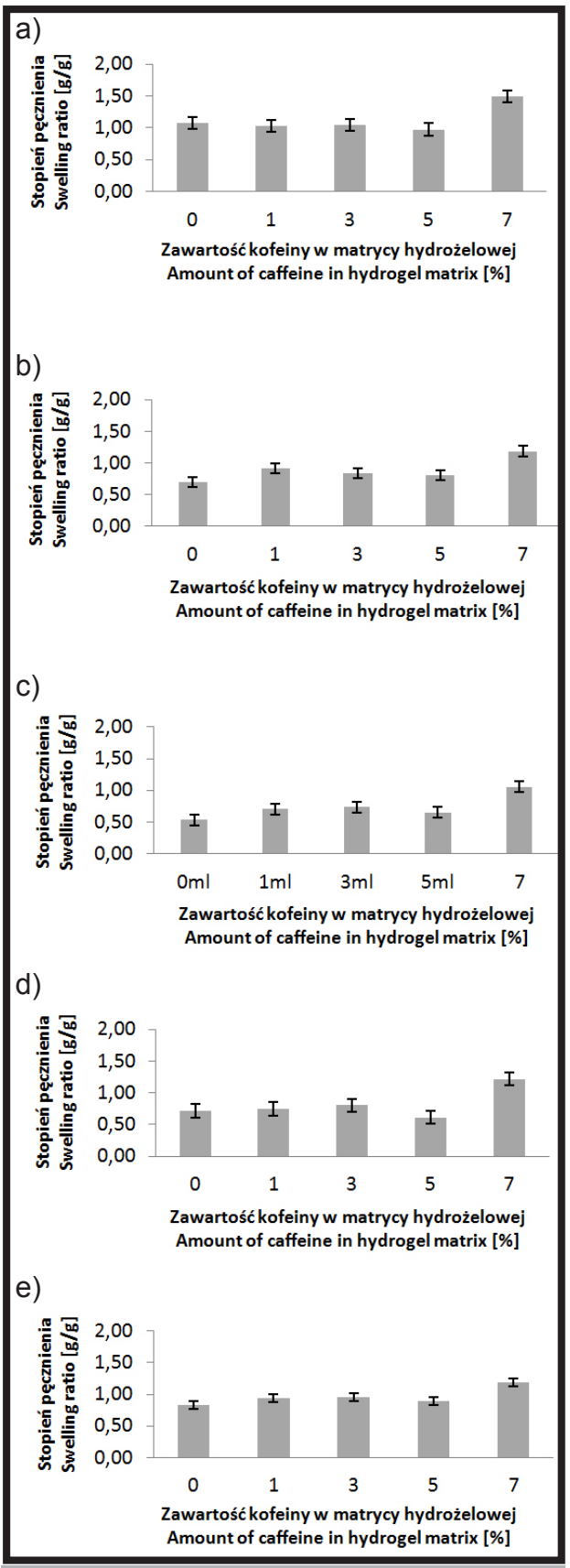

RYS. 1. Zdolności pęcznienia badanych materiałów w: a) wodzie destylowanej, b) 0,9% r-r NaCl, c) 0,9% r-r $MgCl_2$, d) płynie Ringera, e) sztucznej ślinie; liczba powtórzeń n = 3.
FIG. 1. Swelling ability of tested hydrogels in: a) distilled water, b) 0.9% NaCl, c) 0.9% $MgCl_2$, d) Ringer's solution, e) artificial saliva; number of repetitions n = 3.

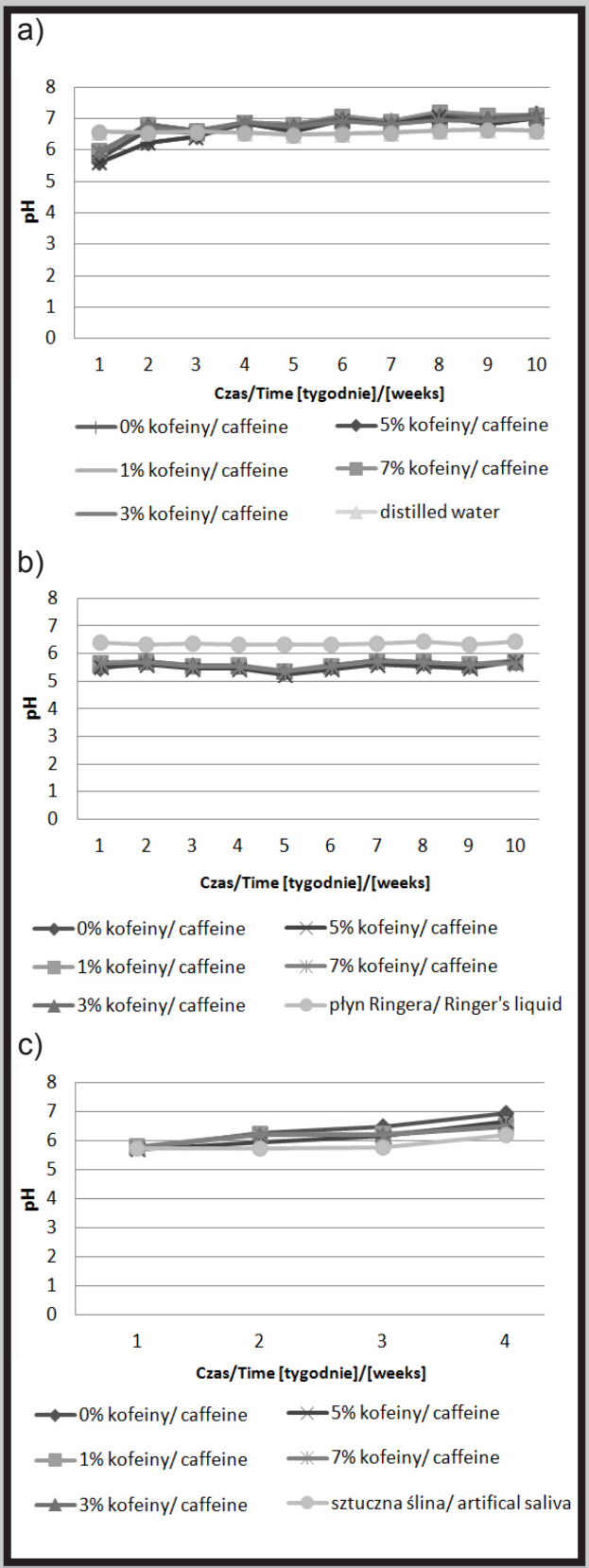

RYS. 2. Zmiany pH: a) wody destylowanej, b) płynu Ringera, c) sztucznej śliny podczas inkubacji przez 10 lub 4 tygodni badanych materiałów hydrożelowych modyfikowanych kofeiną; liczba powtórzeń n = 3.
FIG. 2. Changes in pH values in the following solutions: a) distilled water, b) Ringer's solution, c) artificial saliva during 10 or 4-week incubation of hydrogel materials modified with caffeine; number of repetitions n = 3.

Na podstawie przeprowadzonych badań można stwierdzić, że podatność na pęcznienie materiałów hydrożelowych zmodyfikowanych niewielką ilością roztworu kofeiny – tj. 1, 3 oraz 5% wag.– jest porównywalna do podatności na pęcznienie hydrożelu bez tego dodatku. Dlatego też, można modyfikować taki materiał wymienionymi objętościami roztworu kofeiny, nie zmieniając pojemności sorpcyjnej hydrożeli. W przypadku wprowadzenia do matrycy hydrożelowej 7% wag. roztworu kofeiny obserwuje się wyraźne zwiększenie się zdolności sorpcyjnych badanych materiałów. Prawdopodobnie jest to związane z faktem, że kofeina jest dodawana do materiału hydrożelowego w formie rozcieńczonego roztworu wodnego. Stąd też po wprowadzeniu takiej ilości rozpuszczalnika do układu możliwe jest powstawanie wiązań wodorowych pomiędzy cząsteczkami tego rozpuszczalnika a cząsteczkami rozpuszczalnika obecnego w absorbowanym medium. Na tej podstawie można stwierdzić, że modyfikacja matrycy hydrożelowej za pomocą 7% wag. roztworu kofeiny przyczynia się do zmiany właściwości sorpcyjnych badanych materiałów hydrożelowych.

Badanie inkubacyjne

Badanie inkubacyjne pozwala określić zmiany wartości pH symulowanych płynów ustrojowych, występujących w ludzkim organizmie pod wpływem obecności badanych materiałów. Dzięki temu możemy określić czy inkubacja materiałów może mieć negatywny wpływ na zsyntezowany materiał oraz czy spowoduje zmiany pH zewnętrznego środowiska do wartości niepożądanych - takich, które mogą świadczyć o zachodzeniu procesu degradacji. Na RYS. 2 przedstawiono zmiany wartości pH płynów, w których inkubowano badane materiały.

Zmiany pH płynów w czasie inkubacji w nich materiałów hydrożelowych były niewielkie, co sugeruje, że albo degradacja materiałów w takich warunkach nie zachodzi, albo produkty degradacji nie mają wpływu na pH płynów inkubacyjnych. Jest to badanie wstępne i w przyszłości powinny zostać przeprowadzone bardziej dokładne badania, które odpowiedziałyby na pytanie czy proces degradacji materiałów zachodzi w pierwszych tygodniach ich inkubacji w analizowanych płynach.

Badanie spektroskopowe

Badania FTIR miały na celu sprawdzenie wpływu symulowanych płynów ustrojowych na strukturę analizowanych materiałów. Na RYS. 3-7 zaprezentowano widma FT-IR dla badanych materiałów hydrożelowych. W TABELACH 1 i 2 zestawiono charakterystyczne pasma z powyższych widm oraz przypisano im odpowiednie grupy funkcyjne. Zanalizowano pasma w próbkach niemodyfikowanych, czyli takich bez dodatku kofeiny oraz modyfikowanych kofeiną.

Na RYS. 3 zestawiono widma FTIR dla próbki niemodyfikowanej oraz dla próbek modyfikowanych najmniejszą i największą ilością kofeiny. Widać w nich wyraźnie charakterystyczne pasma w położeniach 1660, 1700 cm^{-1} pochodzące od drgań rozciągających C=O oraz pasma w położeniach ok. 1250 i ok. 700 cm^{-1} pochodzące od drgań grup C-N (walencyjne) i C-H (deformacyjne). RYS. 4-7 przedstawiają widma FT-IR dla badanych materiałów, ale po okresie inkubacyjnym, który trwał dla wody destylowanej i płynu Ringera 10 tyg., natomiast dla sztucznej śliny 4 tyg.

Based on the conducted studies it can be stated that the swelling capacity of hydrogel materials modified with a small amount of caffeine solution – i.e. 1, 3 and 5 wt% - is comparable to the swelling capacity of unmodified hydrogel. Therefore, it is possible to modify hydrogel polymers with the mentioned volumes of caffeine solution without changing their sorption capacity. In the case of introduction of 7 wt% of caffeine solution into the hydrogel matrix, the sorption capacity of the tested materials increased. This is probably due to the fact that caffeine is added in the form of a diluted aqueous solution. Hence, after introduction of such amount of additional solvent into the system, formation of hydrogen bonds between the molecules of these solvent and the solvent molecules present in the absorbed medium can take place. Thus it can be stated that the modification of the hydrogel matrix with 7 wt% caffeine solution contributes to the change of the sorption properties of the tested hydrogel materials.

Incubation studies

The study let us to determine possible changes in pH value of the liquids similar to solutions present in the human body during 10 weeks of incubation. Due to such research it is possible to define whether such long period of incubation can have a negative impact on the synthesized materials (i.e. whether prepared hydrogels cause rapid changes in pH that may indicate that degradation process occurs). In FIG. 2 changes in pH values during incubation of the hydrogels are shown.

The results show that changes in pH of tested samples incubated in different solutions are negligible what may suggest that degradation process does not take place, or it occurs but in a way that does not have any impact on the surrounding liquids. It should be mentioned that this is a preliminary test. Further studies are needed to determine in a more precise way whether process of degradation takes place during the first weeks of incubation in used fluids.

FT-IR spectroscopy

The FTIR studies aimed at determining the impact of simulated body fluids on the structure of the tested materials. In FIGs. 3-7 FT-IR spectra of analysed hydrogel materials are presented. TABLES 1 and 2 present the characteristic bands observed on the spectra with appropriate functional groups. Bands derived from unmodified samples, i.e. those without caffeine, and those modified with this compound were analysed.

In FIG. 3 FTIR spectra of unmodified sample and those samples modified with the smallest and the highest amount of caffeine are shown. Clearly visible bands at 1660 cm^{-1}, 1700 cm^{-1} derived from C = O stretching vibrations as well as bands at 1250 cm^{-1} and approx. 700 cm^{-1} derived from C-N (valence) and C-H (deformation) can be observed. FIGs. 4-7 show FT-IR spectra of the tested materials, but after the incubation period which lasted in the case of distilled water and Ringer's solution 10 weeks, while in the case of artificial saliva - 4 weeks.

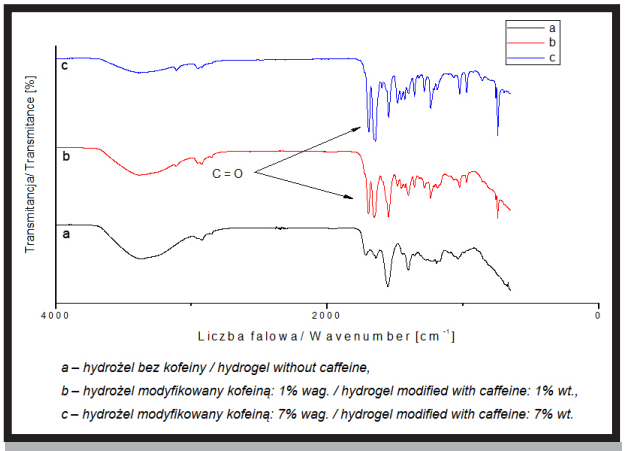

a – hydrożel bez kofeiny / hydrogel without caffeine,
b – hydrożel modyfikowany kofeiną: 1% wag. / hydrogel modified with caffeine: 1% wt.,
c – hydrożel modyfikowany kofeiną: 7% wag. / hydrogel modified with caffeine: 7% wt.

RYS. 3. Widma FT-IR próbek z różną zawartością kofeiny przed inkubacją.
FIG. 3. FT-IR spectra of hydrogel samples with different amount of caffeine before incubation.

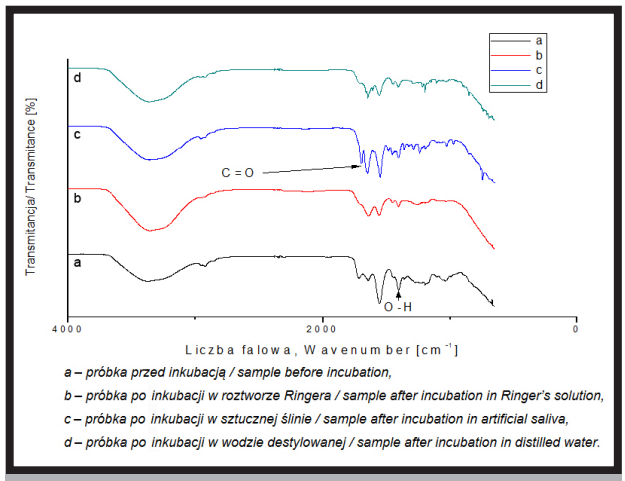

a – próbka przed inkubacją / sample before incubation,
b – próbka po inkubacji w roztworze Ringera / sample after incubation in Ringer's solution,
c – próbka po inkubacji w sztucznej ślinie / sample after incubation in artificial saliva,
d – próbka po inkubacji w wodzie destylowanej / sample after incubation in distilled water.

RYS. 4. Widma FT-IR dla próbki bez kofeiny przed i po inkubacji.
FIG. 4. FT-IR spectra of hydrogel sample without caffeine before and after incubation.

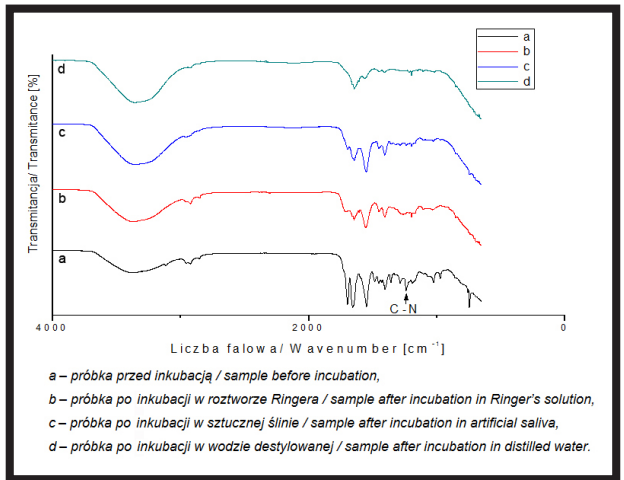

a – próbka przed inkubacją / sample before incubation,
b – próbka po inkubacji w roztworze Ringera / sample after incubation in Ringer's solution,
c – próbka po inkubacji w sztucznej ślinie / sample after incubation in artificial saliva,
d – próbka po inkubacji w wodzie destylowanej / sample after incubation in distilled water.

RYS. 5. Widma FT-IR dla próbki z 1% zawartością kofeiny przed i po badaniu inkubacyjnym.
FIG. 5. FT-IR spectra of hydrogel sample modified with caffeine (1 wt%) before and after incubation.

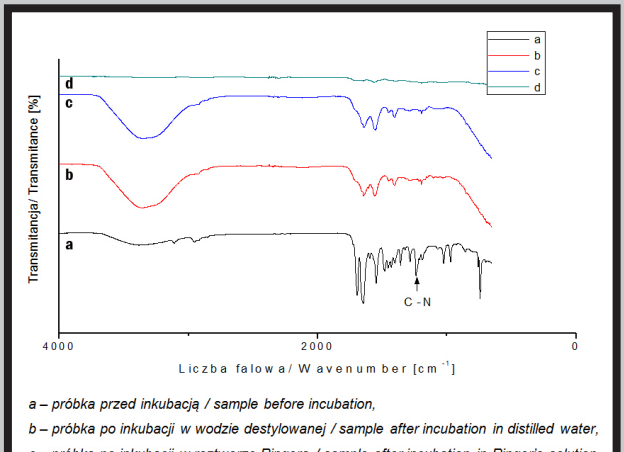

a – próbka przed inkubacją / sample before incubation,
b – próbka po inkubacji w wodzie destylowanej / sample after incubation in distilled water,
c – próbka po inkubacji w roztworze Ringera / sample after incubation in Ringer's solution,
d – próbka po inkubacji w sztucznej ślinie / sample after incubation in artificial saliva.

RYS. 6. Widma FT-IR próbki z 7% zawartością kofeiny przed i po badaniu inkubacyjnym.
FIG. 6. FT-IR spectra of hydrogel sample modified with caffeine (7 wt%) before and after incubation.

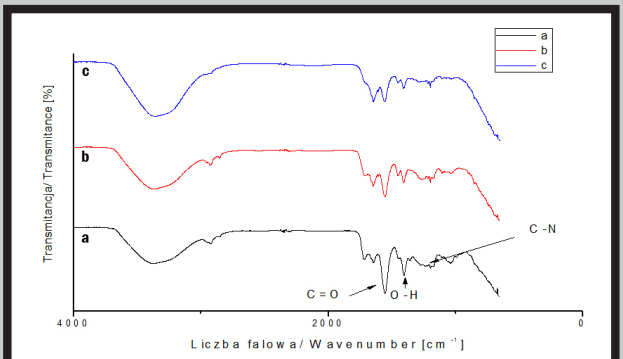

a – hydrożel bez kofeiny / hydrogel without caffeine
b – hydrożel modyfikowany kofeiną: 1% wag. / hydrogel modified with caffeine: 1% wt.
c – hydrożel modyfikowany kofeiną: 7% wag. / hydrogel modified with caffeine: 7% wt.

RYS. 7. Widma FT-IR próbek z różną zawartością kofeiny (1 i 7%) po inkubacji w płynie Ringera.
FIG. 7. FT-IR spectra of hydrogel samples modified with different amount of caffeine (1 and 7 wt%) after incubation in Ringer's solution.

TABELA 1. Charakterystyczne pasma w widmie FT-IR dla próbki materiału bez dodatku kofeiny przed badaniem inkubacyjnym.
TABLE1. Characteristic bands in FT-IR spectrum of sample without caffeine before incubation studies.

Grupa funkcyjna Functional group	Typ drgań Type of vibration	Liczba falowa Wavenumber [cm^{-1}]
O-H	rozciągające / stretching	3350
C-H	rozciągające / stretching	2900
C=O	rozciągające / stretching	1540
O-H	deformacyjne / deformation	1400

TABELA 2. Charakterystyczne pasma w widmach FT-IR dla próbek z dodatkiem 1% i 7% mas. kofeiny przed badaniem inkubacyjnym.
TABLE 2. Characteristic bands in FT-IR spectra in samples modified with 1% and 7% (wt.) caffeine before incubation studies.

Grupa funkcyjna Functional group	Typ drgań Type of vibration	Liczba falowa Wavenumber [cm^{-1}]
O-H	rozciągające / stretching	3350
C-H	rozciągające / stretching	3100
C-H	rozciągające / stretching	2900
C=O	rozciągające / stretching	1650,1700
C=O	rozciągające / stretching	1540
C=C	rozciągające / stretching	1500
C-N	walencyjne / valence	1300
C-H	deformacyjne / deformation	675

Na RYS. 4 przedstawiono widma FT-IR dla próbki niemodyfikowanej kofeiną przed oraz po inkubacji w wyżej wymienionych roztworach. Na widmach obserwujemy mniejszą intensywność pików dla liczb falowych ok. 1250 cm^{-1} od grup O-H pochodzących od kwasu akrylowego. Daje to informację, że może dochodzić do wymywania kwasu akrylowego bądź może to informować o degradacji matrycy poprzez rozpad wiązań polimerowych, w związku z długim procesem inkubacji. Na widmie obserwuje się również pojawienie dodatkowego piku w położeniu ok. 1600 cm^{-1}, który jest charakterystyczny dla grup C=O. Pasmo to pojawia się tylko i wyłącznie dla próbki inkubowanej w sztucznej ślinie. Przyczyną tego jest występowanie w składzie tego roztworu mocznika, który w swojej budowie strukturalnej zawiera właśnie takie grupy funkcyjne.

Na kolejnych wykresach (RYS. 5 i 6) obserwujemy widma FT-IR dla próbki zmodyfikowanej 1% oraz 7% wag. dodatkiem kofeiny, przed oraz po badaniu inkubacyjnym. Obserwujemy zmniejszenie intensywności pasm C-N (1250 cm^{-1}), które świadczą o wypłukiwaniu kofeiny.

Na RYS. 7 zaprezentowano wpływ inkubacji w płynie Ringera na materiały niemodyfikowane i modyfikowane 1% i 7% wag. kofeiny. Im większa zawartość kofeiny w materiale, tym większy zanik pasm takich jak C=O (1550 cm^{-1}), O-H (1400 cm^{-1}) oraz C-N (1300 cm^{-1}). Pasma C=O pochodzą od kofeiny, czynnika sieciującego oraz kwasu akrylowego. Grupy O-H pochodzą wyłącznie od kwasu akrylowego, natomiast pasma od grup C-N pochodzą wyłącznie od kofeiny. Tak więc można stwierdzić, że większa ilość dodatku wpływa na większe rozszerzenie łańcuchów polimerowych w strukturze, a przez to ułatwia to wymywanie kofeiny i być może rozpad łańcuchów polimerowych, czego efektem jest obniżenie intensywności pasm od kwasu akrylowego oraz czynnika sieciującego.

Potwierdzeniem wniosków wysnutych na podstawie tego badania mogą być przeprowadzone w przyszłości badania nad uwalnianiem substancji czynnej z otrzymanych materiałów przeprowadzone w membranach imitujących ludzką skórę.

In FIG. 4 FT-IR spectra of an unmodified sample before and after incubation in the above-mentioned liquids are shown. In the spectra, a low intensity of peaks at approx. 1250 cm^{-1} originating from O-H groups derived from acrylic acid can be noticed. Thus ewe can hypothesise that elution of acrylic acid can occur or degradation of the matrix by the breakdown of polymer bonds due to the long incubation process can take place. In the spectrum an additional peak at approximately 1600 cm^{-1}, which is characteristic for C=O groups also can be observed. This band appears only in the case of the sample incubated in artificial saliva. The reason for this is presence of urea in this liquid, which contains such functional groups in its structure.

In FIGs. 5 and 6 the FT-IR spectra of samples modified with caffeine in an amount of 1% and 7% by weight before and after incubation studies are shown. Decrease in the intensity of C-N bonds (1250 cm^{-1}), which indicates the process of caffeine elution from the tested hydrogel is visible.

In FIG. 7 the impact of incubation in Ringer's solution on unmodified and modified materials with 1% and 7% by weight caffeine is presented. The higher caffeine content in the material resulted in the greater disappearance of bands from groups such as C=O (1550 cm^{-1}), O-H (1400 cm^{-1}) and C-N (1300 cm^{-1}). C=O bands are derived from caffeine, crosslinking agent and acrylic acid. Bands characteristic for O-H groups are derived exclusively from acrylic acid, while the bands from C-N groups are derived exclusively from caffeine. Thus, it can be stated that a higher amount of the additive affects polymer chains in the structure to a higher extent, and thus facilitates elution of caffeine and perhaps the breakdown of bonds in polymer chains, which results in the lower intensity of the bands from acrylic acid and the cross-linking agent.

To confirm this hypothesis additional experiments on the release of the active substance from the obtained materials carried out using membranes imitating human skin will be conducted in the future.

Wnioski

Na podstawie przeprowadzonych badań, możemy stwierdzić, że otrzymane materiały wykazują dobrą zdolność do pęcznienia w symulowanych płynach ustrojowych. Pęcznienie tych materiałów zależy również od roztworu, w którym dokonywano badania, a nie tylko od matrycy. Obecność różnych jonów w medium inkubacyjnycm ma duży wpływ na pojemności sorpcyjne badanych materiałów, tak więc materiały te w środowisku wody destylowanej pęcznieją najbardziej. W przypadku roztworów takich jak sztuczna ślina, płyn Ringera czy roztwory $MgCl_2$ oraz NaCl obserwuje się mniejsze pęcznienie, a jest to spowodowane występowaniem dużej ilości jonów w tych roztworach. Ponadto, warto również zaznaczyć, że znaczenie ma również wartościowość jonów, co możemy obserwować porównując pęcznienie tych materiałów w obecności jonów Na^+ oraz Ca^{2+}. Obecność w płynie jonów dwuwartościowych powoduje wzrost usieciowania struktury, a tym samym wpływa na zmniejszenie pojemności sorpcyjnej takiego materiału. Różnica w pęcznieniu była również widoczna dla materiału zmodyfikowanego największą ilością dodatku, tj. 7% wag. Tak więc badanie to dostarcza informacji o możliwości regulacji pojemnością sorpcyjną tych materiałów, poprzez zastosowanie odpowiedniej ilości czynnika modyfikującego, bądź w zależności od środowiska, w którym będzie stosowany.

Ponadto, badanie materiały podczas badania inkubacyjnego, trwającego 10 tygodni nie powodowały zmian pH w roztworach. Podczas pomiarów nie obserwowano znacznych spadków oraz skoków w wartościach pH, co może świadczyć o ich stabilności. Na podstawie badań FTIR stwierdzono, że inkubacja w badanych płynach wpływa na uwalniane kofeiny, ponieważ obserwuje się na widmach zmniejszenie lub zanik charakterystycznych pasm, które są obecne w materiale przed badaniem.

Podziękowania

Badanie finansowane były w ramach projektu C-4/439/2017/DS.

Conclusions

Based on the conducted studies we can conclude that obtained materials show good swelling capacity in simulated body fluids. The swelling of these materials depends on the composition of the hydrogel matrix but also on the fluid in which the study was conducted. The presence of various ions in the incubation medium has a major impact on the sorption capacity of the tested materials; therefore these materials swell the most in distilled water. In the case of solutions such as artificial saliva, Ringer's solution or solutions of $MgCl_2$ and NaCl, a lower swelling is observed, which is caused by the presence of a large amount of ions in these liquids. In addition, it is also worth noting that the type of ions is also important, which can be observed by comparison of the swelling of these materials in the presence of Na^+ and Ca^{2+} ions. The presence of divalent ions in the tested medium causes an increase in cross-linking degree of hydrogel structure, and thus reduces the sorption capacity of such material. The difference in swelling properties was also visible in the case of the material modified with the highest amount of the additive, i.e. 7 wt%. Thus, the study provides information on the possibility of adjusting the sorption capacity of these materials by using an appropriate amount of the modifying agent, or depending on the environment in which it will be used.

In addition, analysed materials during the incubation study that lasted 10 weeks did not cause any significant changes in pH of the tested liquids. During the measurements, any significant decreases in pH values were observed, which may indicate stability of the materials. Based on FTIR analysis it can be stated that incubation in the tested liquids affects the release of caffeine, because in the spectra less intensity or even disappearance of bands characteristic for particular functional groups present in the material before the study can be observed.

Acknowledgements

The research was supported by grant C-4/439/2017/DS.

Piśmiennictwo

[1] Gupta P., Vermani K., Garg S.: Hydrogels: from controlled release to pHresponsive drug delivery. Drug Discov Today 10 (2002) 569-578.
[2] Pluta J., Koralewicz B.: Hydrożele: właściwości i zastosowanie w technologii postaci leku. II. Możliwości zastosowania hydrożeli jako nośników substancji leczniczej. Polimery w Medycynie 3 (2004) 3-19.
[3] Enrica C., Vitaliy V.K.: Biomedical applications of hydrogels: A review of patents and commercial products. European Polymer Journal 65 (2015) 252-267.
[4] Gibas I., Janik H.: Review: Synthetic Polymer Hydrogels for Biomedical applications. Chemistry & Chemical Technology 4 (2010) 297-304.
[5] Rabek J.F.: Polimery, Polskie Wydawnictwo Naukowe, Warszawa 2013.
[6] Andrzejewska E., Marcinkowska A., Podgórska M., Stępniak I., Sydej M.: Photopolymeryzation. New inwestigationes. New Materials. Polimery 5 (2009) 325-404.
[7] Tyliszczak B., Drabczyk A., Kudłacik S.: Comparison of Hydrogels Based on Commercial Chitosan and Beetosan® Containing Nanosilver. Molecules 22 (2017) 61.
[8] Tyliszczak B., Drabczyk A., Kudłacik S., Sobczak-Kupiec A.: Beetosan®-Based Hydrogels Modified with Natural Substances. Journal of Renewable Materials 5 (2017) 174-179.

References

[9] Tyliszczak B., Drabczyk A., Kudłacik S., Sobczak-Kupiec A.: Preparation, characterization, and in vitro cytotoxicity of chitosan hydrogels containing silver nanoparticles. Journal of Biomaterials Science, Polymer Edition 28 (2017) 1665-1676.
[10] Pires-de-Campos M., Leonardi G., Chorilli M.: The effect of topical caffeine on the morphology of swine hypodermis as measured by ultrasound. Journal of Cosmetic Dermatology 7 (2008) 232-237.
[11] Shakeel F., Faisal M.S.: Caffeine: A potential complexing agentfor solubility and dissolution enhancement of celecoxib. Pharmaceutical Biology 48 (2010) 113-115.
[12] Jagoda A.: Caffeine as an indicator of anthropogenic contamination of the water environment, Rozprawa doktorska, Politechnika Krakowska, Kraków 2014.
[13] Fredholm B.: Methyloxantines, Springer, Berlin 2011.
[14] Andreeva E., Dmitrienko S.G., Zolotov A.: Methylxanthines: properties and determination in various objects. Russian Chemical Reviews 81 (2012) 397-414.
[15] Bellisle F., Blundel J.E. , Dye L., Fantino M., Fern E., Fletchee R.J., Lambed J., Roberfroid M., Specter S., Westenhofer J.: Functional food science and behaviour and psychological functions. British Journal of Nutrition 1 (1998) 173-193.
[16] Gugino B.K., Idowu O.J., Schindelbeck H.M., van Es H.M., Wolfe D.W., Thies J.E., Abawi G.S.: Cornell soil health assessment training manual, NYSAES, Geneva, New York 2007.

STUDIA PODYPLOMOWE
Biomateriały – Materiały dla Medycyny
2017/2018

Organizator: Akademia Górniczo-Hutnicza im. Stanisława Staszica w Krakowie Wydział Inżynierii Materiałowej i Ceramiki Katedra Biomateriałów **Kierownik:** prof. dr hab. inż. Elżbieta Pamuła **Sekretarz:** dr inż. Małgorzata Krok-Borkowicz	**Adres:** 30-059 Kraków, Al. Mickiewicza 30 Pawilon A3, p. 208, 210 lub 501 tel. 12 617 44 48, 12 617 23 38, fax. 12 617 33 71 email: epamula@agh.edu.pl; krok@agh.edu.pl http://www.agh.edu.pl/ksztalcenie/oferta-ksztalcenia/studia-podyplomowe/biomaterialy-materialy-dla-medycyny/

Charakterystyka:
Tematyka prezentowana w trakcie zajęć obejmuje przegląd wszystkich grup materiałów dla zastosowań medycznych: metalicznych, ceramicznych, polimerowych, węglowych i kompozytowych. Słuchacze zapoznają się z metodami projektowania i wytwarzania biomateriałów a następnie możliwościami analizy ich właściwości mechanicznych, właściwości fizykochemicznych (laboratoria z metod badań: elektronowa mikroskopia skaningowa, mikroskopia sił atomowych, spektroskopia w podczerwieni, badania energii powierzchniowej i zwilżalności) i właściwości biologicznych (badania: *in vitro* i *in vivo*). Omawiane są regulacje prawne i aspekty etyczne związane z badaniami na zwierzętach i badaniami klinicznymi (norma EU ISO 10993). Słuchacze zapoznają się z najnowszymi osiągnięciami w zakresie nowoczesnych nośników leków, medycyny regeneracyjnej i inżynierii tkankowej.

Sylwetka absolwenta:
Studia adresowane są do absolwentów uczelni technicznych (inżynieria materiałowa, technologia chemiczna), przyrodniczych (chemia, biologia, biotechnologia) a także medycznych, stomatologicznych, farmaceutycznych i weterynaryjnych, pragnących zdobyć, poszerzyć i ugruntować wiedzę z zakresu inżynierii biomateriałów i nowoczesnych materiałów dla medycyny. Słuchacze zdobywają i/lub pogłębiają wiedzę z zakresu inżynierii biomateriałów. Po zakończeniu studiów wykazują się znajomością budowy, właściwości i sposobu otrzymywania materiałów przeznaczonych dla medycyny. Potrafią analizować wyniki badań i przekładać je na zachowanie się biomateriału w warunkach żywego organizmu. Ponadto słuchacze wprowadzani są w zagadnienia dotyczące wymagań normowych, etycznych i prawnych niezbędnych do wprowadzenia nowego materiału na rynek. Ukończenie studiów pozwala na nabycie umiejętności przygotowywania wniosków do Komisji Etycznych i doboru metod badawczych w zakresie analizy biozgodności materiałów.

Zasady naboru:
Termin zgłoszeń: od 20.09.2017 do 20.10.2017 (liczba miejsc ograniczona - decyduje kolejność zgłoszeń)
Wymagane dokumenty: dyplom ukończenia szkoły wyższej
Osoby przyjmujące zgłoszenia:
prof. dr hab. inż. Elżbieta Pamuła (pawilon A3, p. 208, tel. 12 617 44 48, e-mail: epamula@agh.edu.pl)
dr inż. Małgorzata Krok-Borkowicz (pawilon A3, p. 210, tel. 12 617 23 38, e-mail: krok@agh.edu.pl)

Czas trwania: 2 semestry (od XI 2017 r. do VI 2018 r.) 8 zjazdów (soboty-niedziele) 1 raz w miesiącu	**Opłaty:** 2 600 zł